

# **In Situ Stress at the Lucky Friday Mine**

**(In Four Parts)**

**2. Analysis of Overcore Measurement  
From 5300 Level**

**UNITED STATES DEPARTMENT OF THE INTERIOR**



**UNITED STATES BUREAU OF MINES**

*U.S. Department of the Interior  
Mission Statement*

As the Nation's principal conservation agency, the Department of the Interior has responsibility for most of our nationally-owned public lands and natural resources. This includes fostering sound use of our land and water resources; protecting our fish, wildlife, and biological diversity; preserving the environmental and cultural values of our national parks and historical places; and providing for the enjoyment of life through outdoor recreation. The Department assesses our energy and mineral resources and works to ensure that their development is in the best interests of all our people by encouraging stewardship and citizen participation in their care. The Department also has a major responsibility for American Indian reservation communities and for people who live in island territories under U.S. administration.

**Report of Investigations 9560**

# **In Situ Stress at the Lucky Friday Mine**

**(In Four Parts)**

## **2. Analysis of Overcore Measurement From 5300 Level**

**By J. K. Whyatt, F. M. Jenkins, and M. K. Larson**

**UNITED STATES DEPARTMENT OF THE INTERIOR  
Bruce Babbitt, Secretary**

**BUREAU OF MINES  
Rhea Lydia Graham, Director**

International Standard Serial Number  
ISSN 1066-5552

## CONTENTS

Page

Abstract . . . . .	1
Introduction . . . . .	2
Field measurement . . . . .	2
Overcore method . . . . .	7
Site geology . . . . .	10
Mining experience . . . . .	10
Stress field estimate . . . . .	14
Evaluation of strain data . . . . .	14
Stress field solution . . . . .	16
Stress field characterization . . . . .	18
Doorstopper-scale assumptions . . . . .	18
Site-scale assumptions . . . . .	18
Local stress variability . . . . .	18
Sampling . . . . .	25
Discussion and conclusions . . . . .	26
Acknowledgments . . . . .	27
References . . . . .	27
Appendix A.—Mining-induced stress at overcore site . . . . .	29
Appendix B.—Drilling notes on geology . . . . .	30
Appendix C.—Rock properties . . . . .	31
Appendix D.—Rock-burst elastic energy release . . . . .	32
Appendix E.—Doorstopper cell local solutions . . . . .	33

## ILLUSTRATIONS

1. Location of Lucky Friday Mine . . . . .	3
2. Plan view of 5300-level site and vicinity . . . . .	4
3. Vertical section of 5300-level site showing excavation state during measurement . . . . .	5
4. Detailed plan view of 5300-level site . . . . .	6
5. Overcore measurement sites . . . . .	8
6. Schematic of CSIR doorstopper cell in borehole . . . . .	9
7. Tested sections, geologic formation, and stress solution at 5300-level site . . . . .	11
8. Damage caused by rock burst on January 17, 1990 . . . . .	12
9. Crosscut after removal of debris from January 17, 1990, rock burst . . . . .	13
10. Local stress field on end of borehole for each doorstopper cell . . . . .	20
11. Local stress field on end of borehole summarized from results plotted in figure 10 . . . . .	24

## TABLES

1. Overcore borehole orientations . . . . .	2
2. Results of overcore measurements with doorstopper cells . . . . .	7
3. Estimated rock properties . . . . .	10
4. Ranking criteria for quality designation . . . . .	14
5. Measurement quality as classified by range screen . . . . .	15
6. Measurement quality as classified by strain screen . . . . .	15
7. Comparison of screen results . . . . .	16
8. Stress field estimates . . . . .	17
9. Best estimate of stress field in map coordinate system . . . . .	17
10. Location and number of good outlying overcore strain measurements . . . . .	19

## TABLES—Continued

	<i>Page</i>
11. Stress estimates exploring good outlying strain measurements .....	19
12. Stress estimates developed from strain-screened data from various combinations of three of four boreholes .....	23
13. Stress estimates from high stress and average stress data sets .....	25
14. Best estimate of average stress conditions at measurement site .....	26
A-1. Mining-induced stress at measurement site .....	29
C-1. Rock type and results of uniaxial compression tests .....	31
C-2. Measured rock properties of sulfide-altered quartzite, 4250 level, Lucky Friday Mine .....	31
C-3. Properties of Revett Formation rocks from various locations in Coeur d'Alene Mining District .....	31
E-1. Principal stress solutions for stress on end of borehole .....	33
E-2. Range of individual doorstopper cell solutions for stress on end of borehole .....	34

### UNIT OF MEASURE ABBREVIATIONS USED IN THIS REPORT

#### Metric Units

cm	centimeter	MJ/m <sup>3</sup>	megajoule per cubic meter
deg	degree	mm	millimeter
g/cm <sup>3</sup>	gram per cubic centimeter	MPa	megapascal
GPa	gigapascal	pct	percent
km	kilometer	t	metric ton
m	meter	t/m <sup>3</sup>	metric ton per cubic meter
m <sup>3</sup>	cubic meter	μ $\epsilon$	microstrain
MJ	megajoule	°C	degree Celsius

#### U.S. Customary Units

ft	foot	psi	pound per square inch
ft <sup>3</sup>	cubic foot	st	short ton
in	inch	°F	degree Fahrenheit

Reference to specific products does not imply endorsement by the U.S. Bureau of Mines.

# IN SITU STRESS AT THE LUCKY FRIDAY MINE

(In Four Parts)

## 2. Analysis of Overcore Measurement From 5300 Level

By J. K. Whyatt,<sup>1</sup> F. M. Jenkins,<sup>1</sup> and M. K. Larson<sup>1</sup>

---

### ABSTRACT

The U.S. Bureau of Mines conducted an overcore stress measurement on the 5300 level of the Lucky Friday Mine, Mullan, ID, to investigate the stress regime around an experimental stope in a rock-burst-prone mine. The result indicated a stress field with unexpected magnitude and orientation [ $\sigma_1 \approx 135$  MPa (19,600 psi) oriented S 80° W]. An unusual amount of rock-burst activity was encountered during subsequent excavation. A careful review of the overcore data suggested the overcore strain measurements were valid. Moreover, concentrated rock-burst activity suggested that the measured stress field did exist, but was localized and therefore did not represent the far-field in situ stress field.

---

<sup>1</sup>Mining engineer, Spokane Research Center, U.S. Bureau of Mines, Spokane, WA.

## INTRODUCTION

The in situ stress measurement described in this Report of Investigations (RI) was undertaken as part of a field trial of an underhand longwall mining method for mechanized mining of rock-burst-prone ground. The U.S. Bureau of Mines (USBM) conducted this study as part of its rock-burst safety research program. The trial took place in a stope, known as the Lucky Friday underhand longwall (LFUL) stope, at the Lucky Friday Mine in the Coeur d'Alene Mining District of northern Idaho (figure 1). This mine has a long history of rock-burst activity (McMahon, 1988), and the underhand longwall method was specifically designed to control rock bursting in mine pillars.<sup>2</sup>

This measurement was undertaken between October 1986 and January 1987 to improve the existing estimate of in situ stress in the Coeur d'Alene Mining District (Whyatt, 1986), which in turn would be used in an analysis of the LFUL stope. However, an examination of the measurement data indicated a stress field significantly different from previous measurements, especially a similar one undertaken by Allen (1979) on the 4250 level of the same mine, and estimates of overburden stress. The unexpected results of the 5300-level measurement cast doubt on its accuracy. Further examination of these discrepancies led to the recognition that there were significant shortcomings in the analytical techniques applied to earlier stress measurements in the district and that furthermore, significant errors existed in some stress estimates.

This erosion of confidence in existing in situ stress information led to a reanalysis of the measurement from the 4250 level, which is reported in part 1 of this series

(Whyatt and Beus, 1995). The resulting reanalysis provided a modified estimate of in situ stress magnitude, but in general, confirmed stress orientation. It also suggested that the measurement site was not as homogeneous as previously assumed.

While the stress field in the Coeur d'Alene Mining District was being reexamined, the LFUL stope was developed as planned. An investigation of the ground control aspects of LFUL stope performance has been completed (Pariseau and others, 1992; Scott, 1993; Whyatt and others, 1992a; Whyatt and others, 1992b; Williams and others, 1992), based on the existing knowledge of in situ stress in the district. During the interim, excavation continued at the 5300-level measurement site, setting off heavy rock-burst activity. The bursts severely damaged the opening and forced its abandonment, lending credence to the accuracy of the 5300-level stress measurement.

This report, the second in a series covering measurement and interpretation of in situ stress at the Lucky Friday Mine, is limited to description and analysis of the stress measurement at the 5300 level. The first report (Whyatt and Beus, 1995) provides an updated reanalysis of an overcore measurement obtained on the 4250 level of the Lucky Friday Mine. The third report (Whyatt and others, 1995a) provides a reanalysis of an overcore measurement from the nearby Star Mine. The final report [part 4 (Whyatt and others, 1996b)] seeks to integrate these overcore measurements of in situ stress with other indications of stress field orientation into an overview of the mine-wide in situ stress field.

## FIELD MEASUREMENT

Site-selection criteria for this stress measurement were very similar to Allen's (1979) when he chose his site on the 4250 level (reviewed in the first report of this series), except that a location in the vicinity of the experimental LFUL stope was desired. The common criteria included finding competent rock to provide adequate diamond drill core recovery in a mine notorious for poor core recovery and avoiding mining-induced stress to provide a clear picture of the natural in situ stress state.

The end of the 101 crosscut stub on the 5300 level was chosen as the measurement site. This site was about 45 m

(150 ft) from the vein and 60 m (200 ft) below active mining (figures 2-3). Mining-induced stress was estimated at less than 5 pct of in situ levels (appendix A). The crosscut was sufficiently developed to allow future extension without interfering with haulage operations but was far short of its planned length.

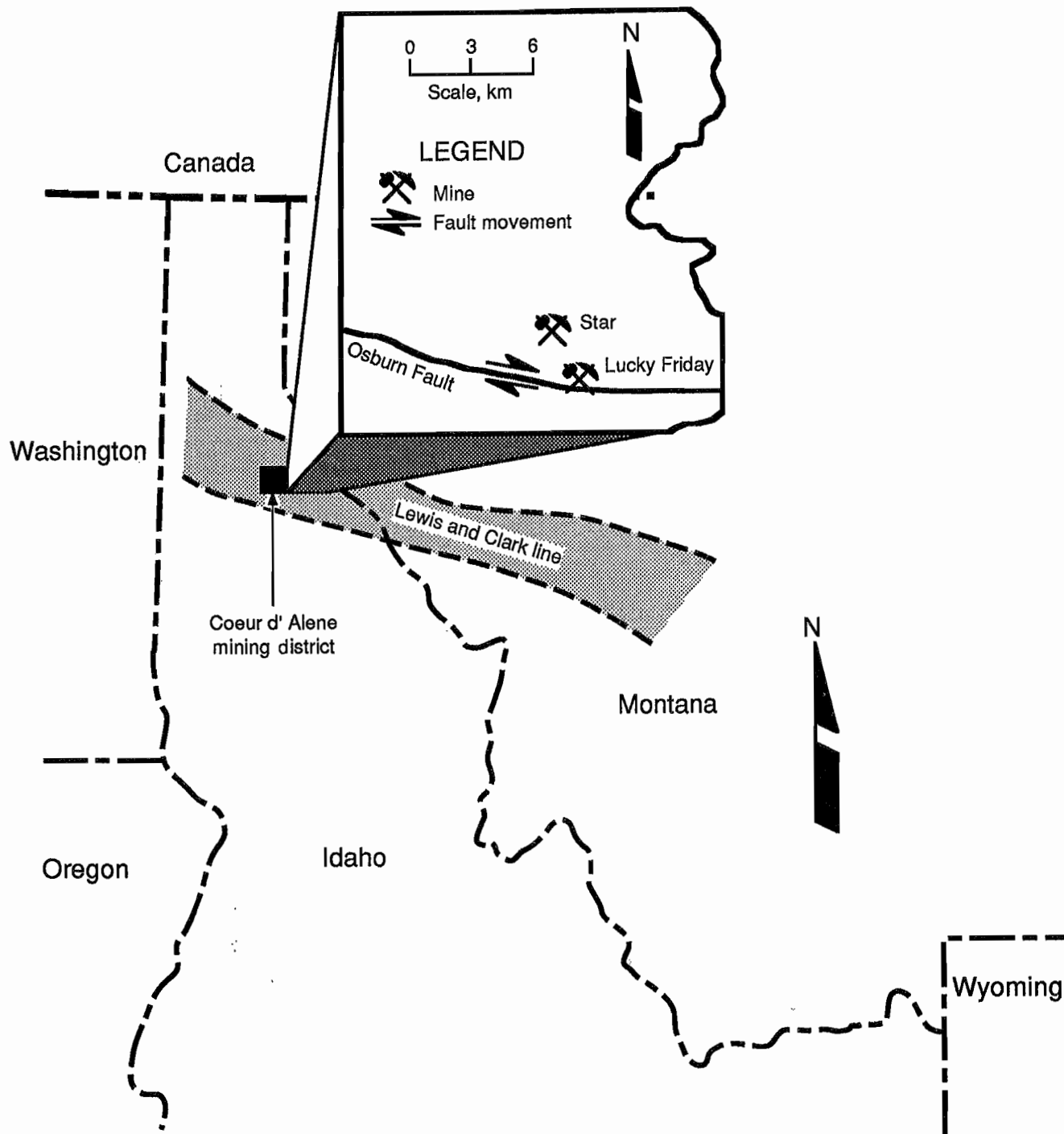
The crosscut stub was mapped for geologic structure, and four boreholes were laid out (figure 4).

Table 1.—Overcore borehole orientations

Borehole	Azimuth, deg	Dip, deg
1 . . . . .	126.4	-3.5
2 . . . . .	216.5	-71.0
3 . . . . .	173.0	-4.5
4 . . . . .	80.5	-2.7

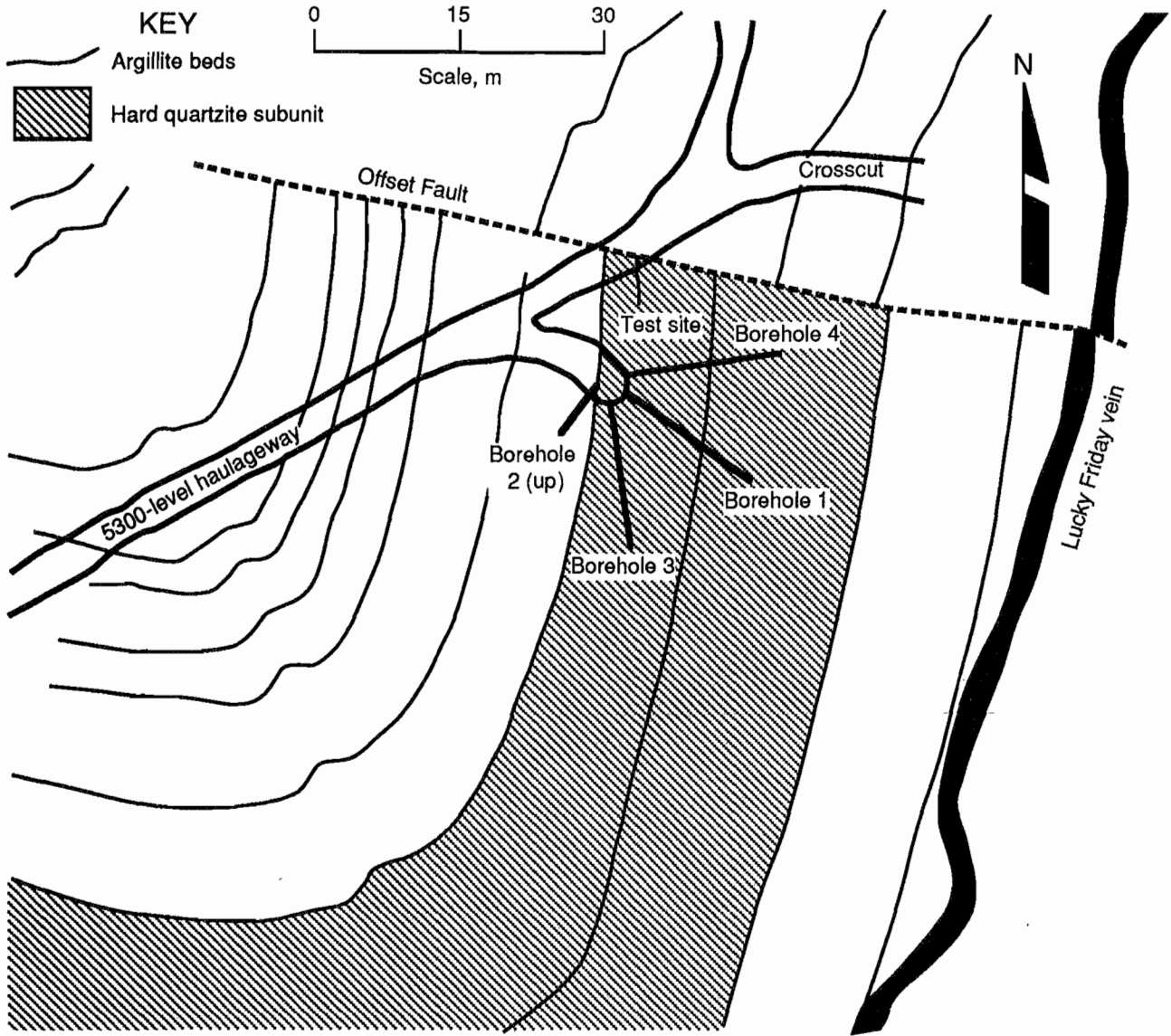
<sup>2</sup>This design was described in a paper, "Underhand Stoping at the Lucky Friday Mine," by R. R. Noyes, G. R. Johnson, and S. D. Lautenschlager, presented at the 94th annual meeting of the Northwest Mining Association, Dec. 2, 1988, in Spokane, WA.

Figure 1



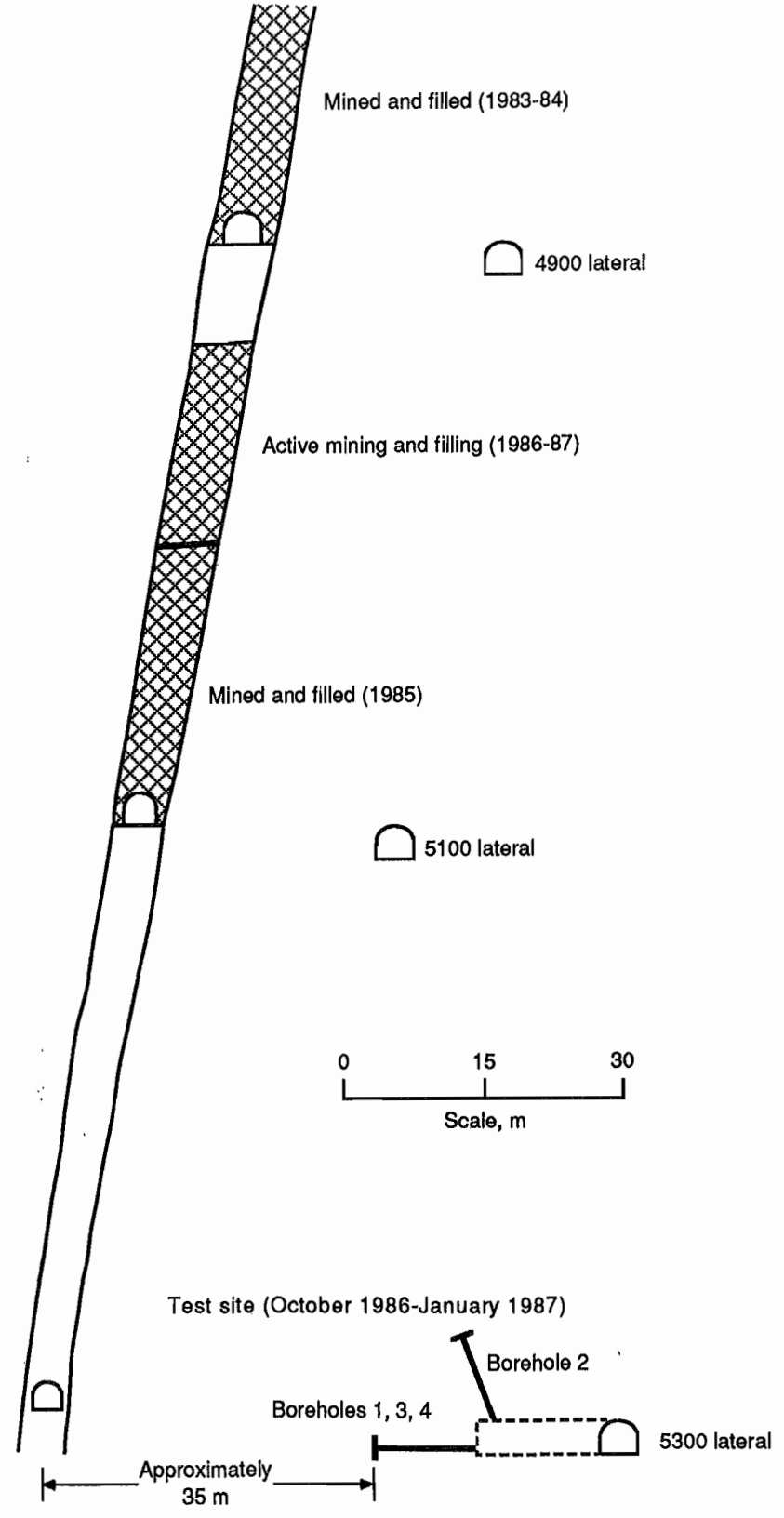
Location of Lucky Friday Mine.

Figure 2



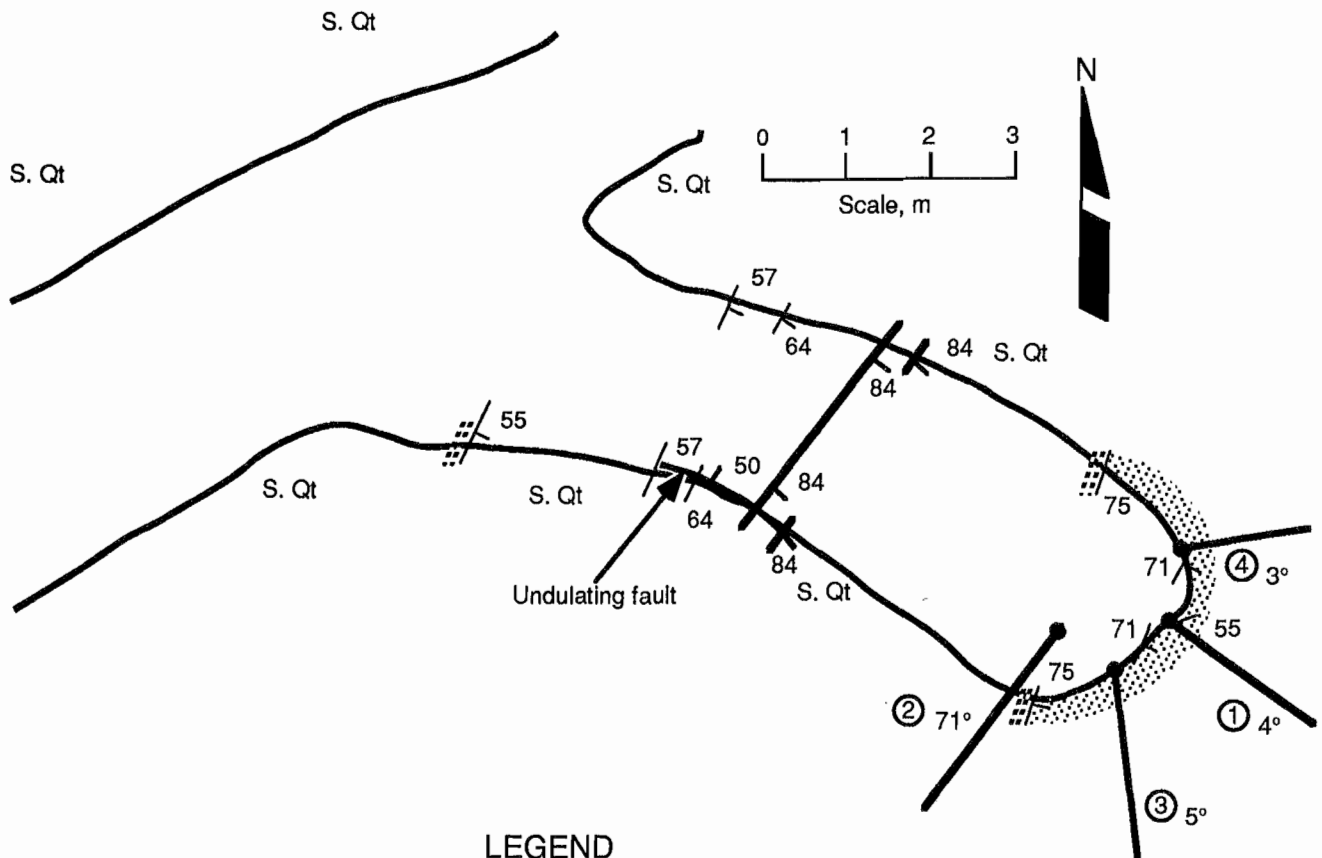
Plan view of 5300-level site and vicinity.

Figure 3



Vertical section of 5300-level site showing excavation state during measurement.

Figure 4



LEGEND

- S. Qt                      Massive, tan-to-brown sericitic quartzite
- .....                    Thin-bedded, light green-to-dark green, metamorphosed argillite.  
(Beds are 1-1/4 to 46 cm thick.)
- .....                    Massive blue-to-tan vitreous quartzite with about 1 pct disseminated sulfides
- 50 |                        Fault showing dip
- 64 |                        Strike and dip of bedding
- Drill hole with inclination
- ① 4°

Detailed plan view of 5300-level site.

The horizontal boreholes were drilled with a slight inclination to aid in keeping the boreholes clean and drained. Each borehole was driven through the crosscut's stress concentration zone (approximately one crosscut diameter) before investigators looked for potential doorstopper installation sites. Borehole orientations are listed in table 1 and doorstopper cell locations are shown in figure 5.

### OVERCORE METHOD

The Council for Scientific and Industrial Research (CSIR) biaxial strain cell, commonly known as a doorstopper, was chosen to measure overcoring strains. The doorstopper cell consists of a four-element strain gauge rosette (figure 6) mounted in a waterproof package that is glued to the polished end of a borehole. The cell measures deformations that accompany unloading of the rock as the cell is overcored. This type of cell was chosen because it is particularly well suited for sites where core recovery is a problem, since only about 7.5 cm (3 in) of overcore is needed for a successful measurement (Jenkins and McKibbin, 1986). This method also uses a smaller diameter borehole than alternative methods.

Installation of doorstopper cells was limited to sections of the borehole that produced sufficiently long pieces of core to ensure that successful measurements could be

made. Once a potential location was identified, the end of the borehole was polished to accept the doorstopper cell and inspected with a borehole television camera. The location was eliminated if fractures or other features were observed that would distort stress measurements. This procedure minimized the number of cell installations that were invalidated by the presence of undetected fractures.

The doorstopper cell was not included in the International Society for Rock Mechanics (ISRM) standard test procedures for overcore stress measurements (ISRM, 1987), but the procedure did not deviate significantly from ISRM procedures for similar overcoring instruments or from the manufacturer's recommended procedure. Extensions of these procedures were devised in an effort to improve the accuracy of overcore strain measurements.

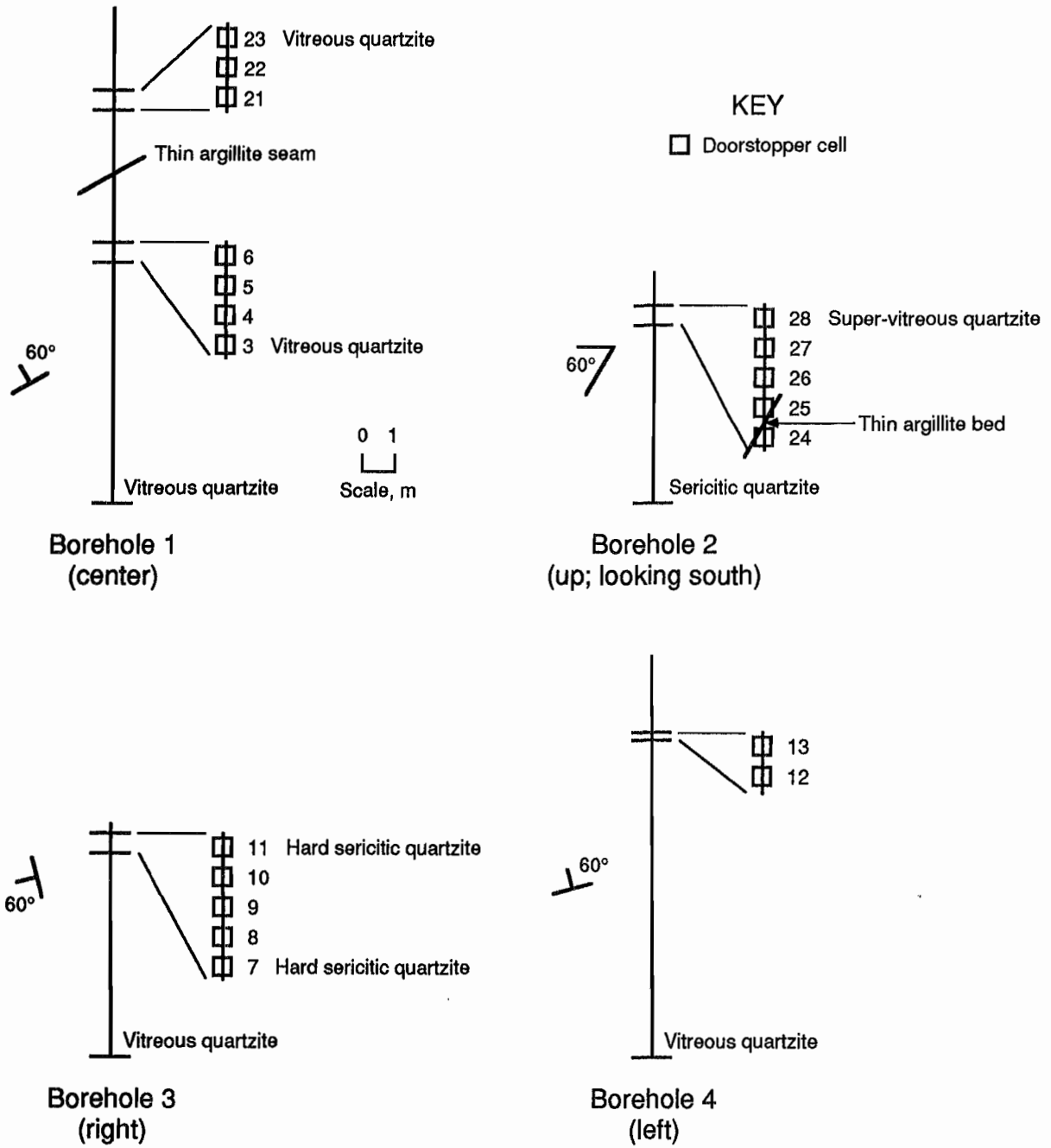
A battery-operated data acquisition system (DAS) was developed to monitor strain through an instrument cable carefully strung through the drill rods, drill head, and water swivel to the DAS. Care had to be taken to maintain a slight amount of tension on the cable during drilling to avoid cable damage. Further details on the DAS, doorstopper cell wiring, and cable routing were reported by Jenkins and McKibbin (1986). This arrangement was used to monitor the complete history of each doorstopper strain gauge during overcoring. The strain changes resulting from overcoring are listed in table 2.

Table 2.—Results of overcore measurements with doorstopper cells

Doorstopper cell	Strain gauge orientation, $\mu\epsilon$				Borehole depth, m	Notes
	+45°	-45°	Vertical	Horizontal		
Borehole 1:						
3	420	927	-369	2,021	7.4	Vitreous quartzite.
4	161	1,856	189	2,127	7.6	
5	146	1,390	-155	2,077	7.7	
6	324	697	508	522	7.9	
21	495	555	503	912	12.2	
22	2,720	958	528	3,798	12.2	
23	666	489	214	885	12.5	Vitreous quartzite.
Borehole 2:						
24	85	1,135	748	587	5.6	Super-vitreous quartzite.
25	483	1,261	1,473	231	5.8	
26	592	2,014	2,097	663	5.9	
27	519	2,441	1,151	1,833	6.0	
28	465	1,383	775	1,092	6.2	
28	465	1,383	775	1,092	6.2	
Borehole 3:						
7	-126	1,764	862	1,007	6.4	Hard sericitic quartzite.
8	1,216	3,871	2,597	2,339	6.5	
9	288	1,928	713	1,136	6.5	Hard sericitic quartzite.
10	618	1,154	940	1,094	6.6	
11	563	148	928	9	6.7	
Borehole 4:						
12	346	1,196	227	1,156	9.8	
13	459	1,631	841	1,709	9.9	

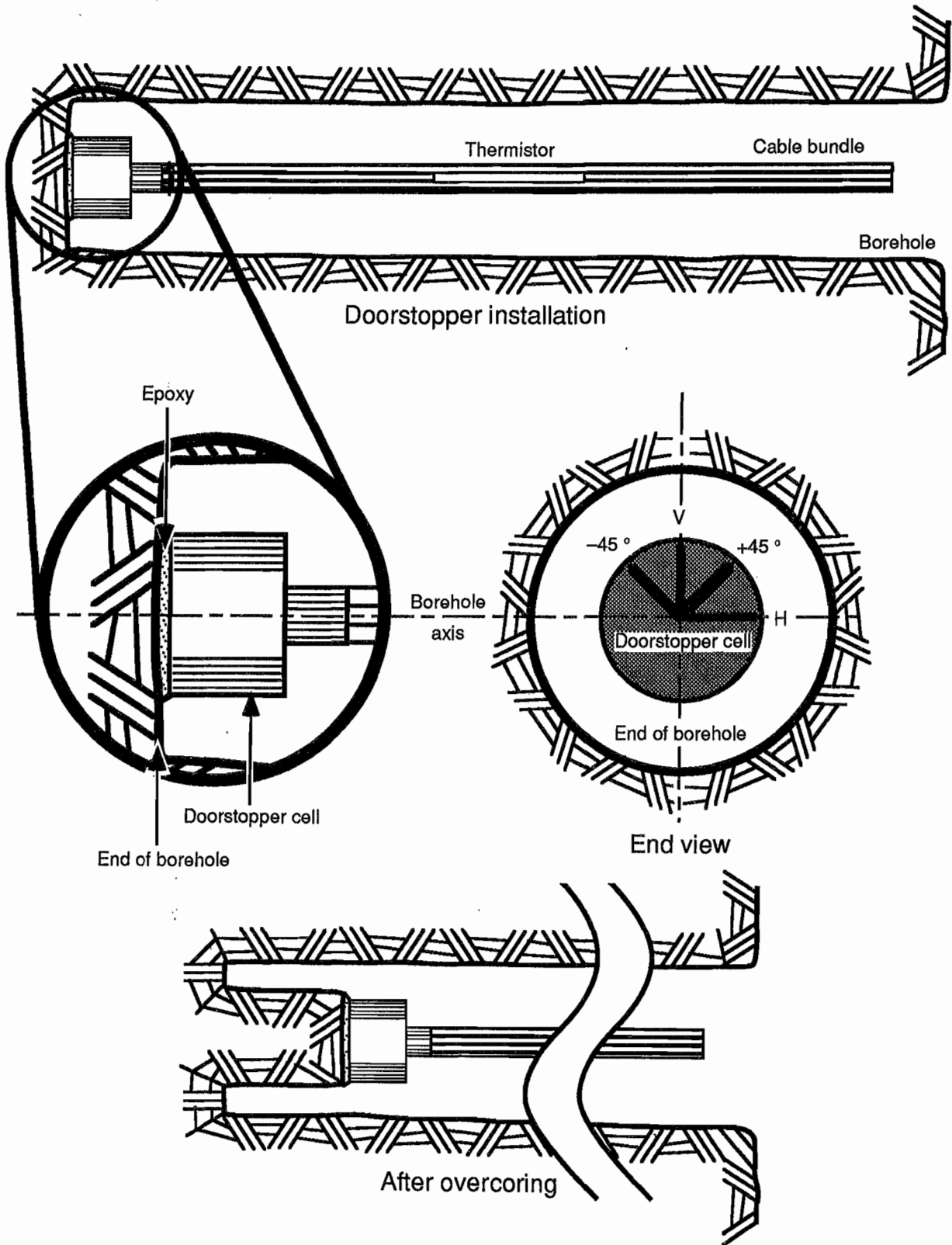
NOTE.—Several doorstopper cells failed and are not included in these results. These were doorstoppers 1 and 2 (glue problems), 15 and 17 (electrical problems), and 16 and 18 (face-polishing problems).

Figure 5



*Overcore measurement sites. Doorstopper cells were not installed in first 5 m of each borehole to minimize influence of excavation-induced stress.*

Figure 6



Schematic of CSIR doorstopper cell in borehole. (H = horizontal; V = vertical.)

The considerable contrast in temperature between mine rock [44 °C (112 °F)] and mine service water [10 °C (50 °F)] at the site raised concerns that the drill water would influence overcore strain measurements. The effect of temperature on strain gauges is widely recognized and has been dealt with in a number of ways. For example, Allen (1979) used a compensating doorstopper cell mounted on a similar piece of rock in his mounting device. However, the cool drill water can also induce thermal strains around the borehole that could distort overcore measurements.

For this measurement, a system was designed to minimize temperature effects by maintaining drill water at rock temperature. A thermistor mounted in the cable bundle just behind the doorstopper cell was used to provide the control signal to a simple heater system that warmed the drill water to rock temperature. Cooling of drill water was accomplished by adding cool mine water. This system was able to maintain the water within about 1 °C (2 °F) of rock temperature (Jenkins and McKibbin, 1986).

### SITE GEOLOGY

The crosscut stub was developed into the edge of a hard quartzite subunit of the Lower Revett Formation (figure 2) to reveal massive, sulfide-altered vitreous quartzite, called "blue rock" by miners. The structure of the subunit, as projected from drilling and nearby openings (see figures 4 and 5 and appendix B), is summarized in figure 7. Rocks in this subunit ranged from hard sericitic quartzite to super-vitreous quartzite. Argillite and softer sericitic quartzites common in other parts of the Revett Formation are generally absent from this subunit.

A number of workers have reported on the elastic properties of Revett quartzites, including Skinner and others (1974), Chan (1972), and Ageton (see report by Beus and Chan, 1980). The most relevant tests were conducted by Allen (1979) on rock samples taken from a vitreous quartzite bed of the Revett at his 4250-level stress measurement site. The original test plan depended on estimates of material properties derived from these earlier studies and assumed fairly uniform geology throughout the measurement site.

The subsequent reanalysis of Allen's (1979) 4250-level measurement showed that variations in properties were systematic within a geologic structure rather than the result of random error. Thus, a program of geologic classification and rock testing was initiated for the 5300 site well after completion of the overcore measurements. Unfortunately, only five doorstopper cells with attached rock core had been saved. These rock samples were classified as hard sericitic quartzite, vitreous quartzite, and

super-vitreous quartzite in order of increasing stiffness and strength. These samples indicated that the overcored portions of boreholes 1, 2, and 3 were drilled in vitreous quartzite, super-vitreous quartzite, and hard sericitic quartzite, respectively (figure 7). Samples from borehole 4 were not available. Elastic properties for these rocks (estimated in appendix C) are summarized in table 3.

Table 3.—Estimated rock properties

Rock type	Young's modulus		Poisson's ratio
	GPa	10 <sup>6</sup> psi	
Hard sericitic quartzite	48	7	0.2
Vitreous quartzite . . . .	69	10	0.1
Super-vitreous quartzite	90	13	0.1
Site average . . . . .	69	10	0.1

### MINING EXPERIENCE

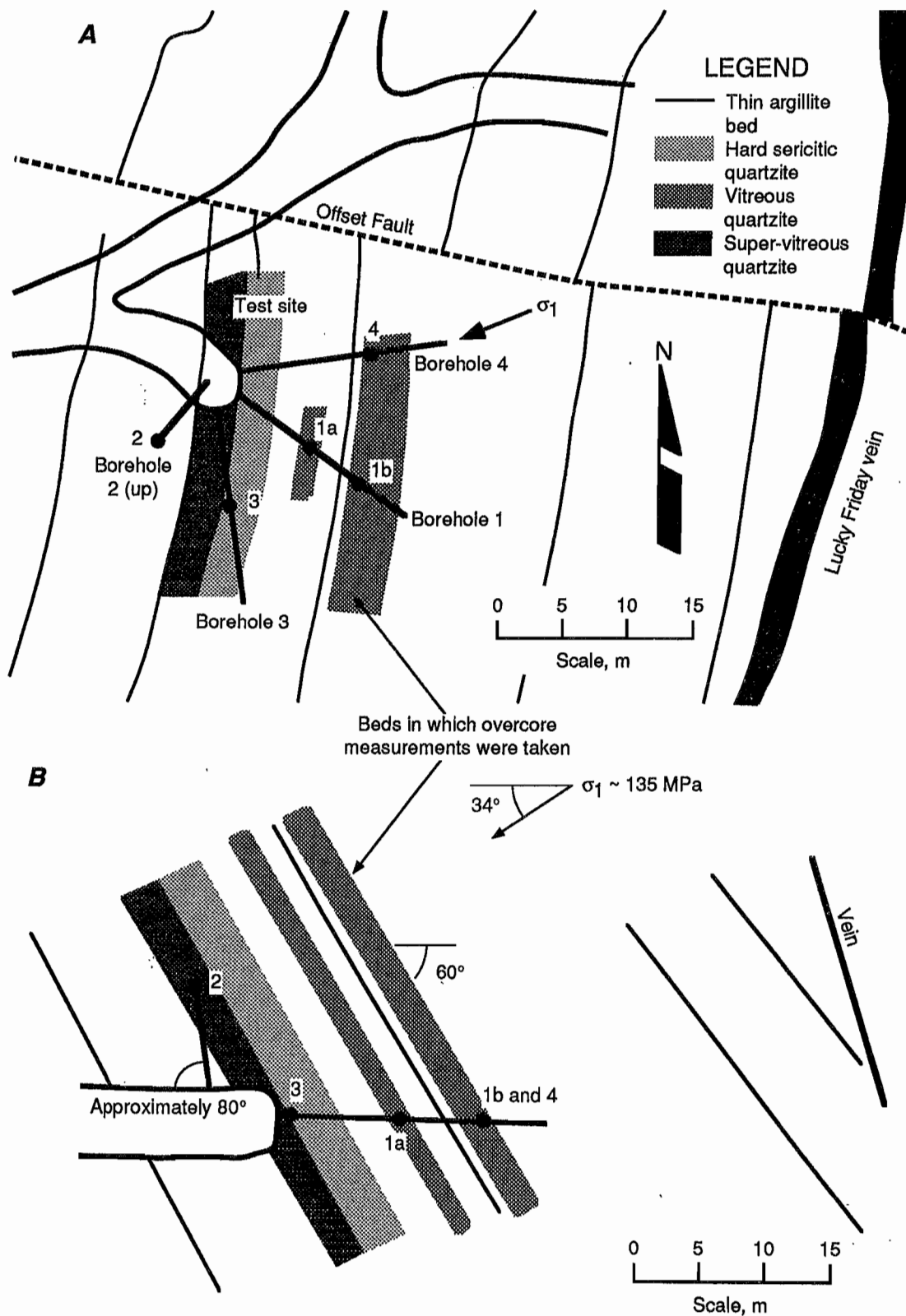
Excavation in the vicinity of the measurement site ceased until the nearby 5210-101 crosscut was developed in November and December 1989. This crosscut was driven approximately 30 m (100 ft) above the measurement site. Shortly thereafter, in January 1990, excavation in the 5300-101 crosscut stub (the stress measurement site) resumed as miners attempted to gain access to the vein.

The first round was taken without incident [approximately 2.5 m (8 ft) of advance], although increased seismic activity was noted. The following round, fired at the end of the day shift on January 10, 1990, triggered a major rock burst measuring 79 mm on the mine's seismograph (a local relative measurement of intensity) with an estimated local magnitude ( $M_1$ ) of 1.4. Forty metric tons (forty-five short tons) of rock collapsed into the 5300-101 crosscut, creating a 2- by 2- by 6-m (6- by 6- by 20-ft) long void in the roof. Another 135 t (150 st) of rock collapsed into the 5210-101 ramp directly above. A map of this damage is provided in figure 8.

After repairs were completed, a third round was shot on January 17, 1990, triggering a burst measuring 31 mm on the mine seismograph and estimated to be less than 1  $M_1$ . This burst took out the right rib of the 5300-101 crosscut, releasing 65 t (72 st) of rock. Subsequent seismic activity continued at high levels. Figure 9 shows the enlarged crosscut after broken rock was removed.

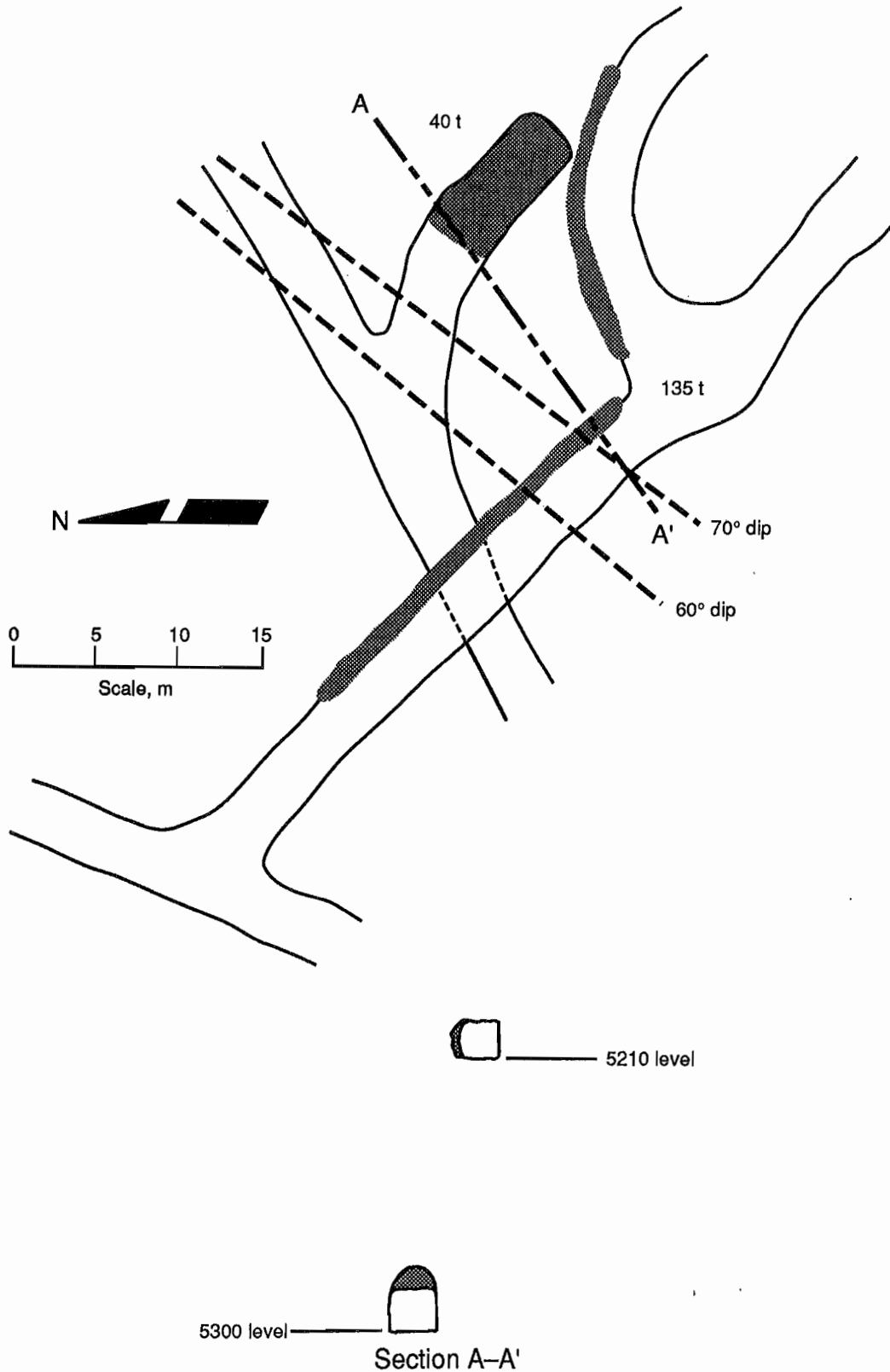
Intense seismic activity continued into the following day, January 18, causing mine personnel to abandon repair activities in the 5300-101 crosscut. Shortly after the crosscut was evacuated, at 8:09 a.m., and without further warning, a rock burst occurred. This rock burst measured 72 mm on the mine seismograph and was estimated at 1.2  $M_1$ . The burst expelled 135 t (150 st) of rock from the right rib

Figure 7



Tested sections, geologic formation, and stress solution at 5300-level site. A, Plan view; B, vertical east-west section.

Figure 8



*Damage (shaded area) caused by rock burst on January 17, 1990.*

Figure 9



*Crosscut after removal of debris from January 17, 1990, rock burst. Original dimensions were 3 by 3 m.*

and back. This burst was particularly dangerous as it occurred on-shift without warning, whereas the previous bursts had occurred with blasting, when the mine was evacuated. Mine management decided to abandon the 5300-101 crosscut after this final burst and to develop an alternative accessway in a safer portion of the rock mass.

The energy released by these three bursts (January 10, 17, and 18, 1990) was not measured directly, but was estimated at 85 to 170 MJ using conventional methods (appendix D). If the source of energy is assumed to be stored elastic strain energy in rock loaded to the measured stress level, these bursts would destress an estimated 86 to 172 m<sup>3</sup> (3,000 to 6,000 ft<sup>3</sup>) of rock, or a sphere between 5.5 and 7 m (18 and 23 ft) in diameter. By comparison, the damage reports estimate that about 375 t (400 st) of

rock collapsed during the three rock bursts. At a laboratory density of 2.7 t/m<sup>3</sup> (see appendix C), this rock has a volume of about 140 m<sup>3</sup> (5,000 ft<sup>3</sup>). Volume and tonnage estimates from the first rock burst suggest a lower in situ density of about 1.9 t/m<sup>3</sup>, which would suggest that about 200 m<sup>3</sup> (7,000 ft<sup>3</sup>) of rock collapsed. Thus, destressing a volume of rock equivalent to the volume of collapsed rock could supply enough energy for the three rock bursts. This implies that only the immediate vicinity of the crosscut was destressed, and it was unlikely that the rock mass was sufficiently destressed to allow completion of the crosscut without additional rock bursts.

Rock bursts are often associated with pockets of highly stressed rock. For instance, Leighton (1982) reported a correlation between high local stresses and rock bursting

in his study of a stope pillar at the nearby Galena Mine. He measured stress in the pillar with vibrating-wire stressmeters as mining narrowed the pillar and concentrated stress in the remnant. The concentration of stress was not uniform. Localized concentrations of stress were built up

during mining and periodically released by a series of rock bursts. The major difference between Leighton's study and this investigation is the relative remoteness of the 5300-101 crosscut measurement site from mining.

## STRESS FIELD ESTIMATE

An accurate estimate of the in situ stress field depends on determining which of the many doorstopper cell measurements were reliable and then applying statistical procedures and accurate stress concentration factors to minimize estimate error. Ideally, the rock mass at the site would be homogeneous and isotropic and would not be influenced by mining. Such an estimate would represent the far-field stress loading mine openings.

Stress estimates were calculated from strain data using the computer program STRESSsOUT (Larson, 1992). STRESSsOUT uses a standard set of assumptions to develop estimates of in situ stress from overcore strain measurements by minimizing the squared error for each strain measurement. By treating all measurements throughout the test site equally, it was assumed that (1) stress and material properties at a site were homogeneous and (2) the rock mass was linearly elastic and had no discontinuities. The program is capable of providing—

1. Statistical treatment of data—A least squares routine ensures equal (or specified) weighting of all data points. This program runs on 8088 or better DOS-based personal computers in a matter of minutes, providing the capability to conduct parametric studies if needed.

2. Improved computations for the induced stress field of a borehole—Advanced modeling techniques have led to the development of more exact stress concentration factors that include the effect of Poisson's ratio. The program uses stress concentration factors specified by the user.

### EVALUATION OF STRAIN DATA

The evaluation of strain data, especially the identification of invalid measurements, is a critical step in estimating the in situ stress field. Field notes describing difficulties with the instruments, bad glue joints, or rock defects are the most important source of information. Further insight can be gained by applying a number of screens that numerically test the overcore strains against various criteria.

A simple screen consists of simply solving for the stress field ( $S_1$ ,  $S_2$ , and  $\theta$ )<sup>3</sup> measured by each of the various sets of three strain gauges in each doorstopper cell and comparing the results. A sound doorstopper overcore measurement should produce substantially the same stress field regardless of which gauges are chosen. Local solutions for the overcore strains shown in table 2 are derived in appendix E. The relative quality of each solution was defined by assigning it to one of five arbitrarily defined groups (table 4) based on the extent of the range of solutions produced (table 5).

Table 4.—Ranking criteria for quality designation<sup>1</sup>

Quality	Maximum percent of variation		
	Orientation <sup>2</sup>	<sup>3</sup> $S_1$	<sup>4</sup> $S_2$
Excellent . . . . .	1	5	5
Good . . . . .	3	10	10
Acceptable . . . . .	5	15	15
Poor . . . . .	10	20	20
Bad . . . . .	>30	>20	>20

<sup>1</sup>See text footnote 3 for explanation of  $S_1$  and  $S_2$ .

$$^2 \frac{\theta_{\max} - \theta_{\min}}{180^\circ} \times 100.$$

$$^3 \frac{S_{1 \max} - S_{1 \min}}{S_{1 \max}} \times 100.$$

$$^4 \frac{S_{2 \max} - S_{2 \min}}{S_{1 \max}} \times 100.$$

A related screen checks for the self-consistency of strain readings in another way. The self-consistency of a doorstopper cell can be tested by determining whether all four

<sup>3</sup> $S_1$  and  $S_2$  are nonstandard notations for the principal stress components on the end of a borehole (standard notations are  $\sigma_1$  and  $\sigma_2$ ). These nonstandard notations are needed to emphasize that they are not far-field in situ stress components. In the equations in table 4, the "min" and "max" subscripts refer to the range of estimates produced. Four estimates are produced by each doorstopper cell.

gauges of a cell are measuring the same strain field. This "strain test" takes advantage of the fact that any two perpendicular measurements of normal strain define the center of a Mohr's circle in strain. Thus, each of two pairs of perpendicular gauges in a doorstopper cell should sum to the same total strain. If the sums are drastically different, the doorstopper cell is failing to measure a single strain field at the end of the borehole. This failure may be attributable to a number of factors, including an electrical fault, the presence of a fracture on or near the face, a poor or nonuniform glue joint, or improper centering of the cell. However, this method will not characterize the source of the strain state, including whether or not isotropic elastic rock is present.

A large difference between the sums for a single cell suggests that the cell should be considered suspect in estimating the in situ stress field. However, defining "large" proved to be problematic. The definition of large was chosen arbitrarily as being a difference greater than either 300  $\mu\epsilon$  or 20 pct of the largest sum. This definition was taken from a reanalysis of the 4250-level measurement in the first RI of this series, where it proved to be convenient. The strain-screening process and resulting strain-screened data set are summarized in table 6. This screen is generally consistent with the first screen, except for doorstopper 10, which passes this screen, while failing the first (table 7).

Table 5.—Measurement quality as classified by range screen<sup>1</sup>

Doorstopper cell	Percent of variation			Quality <sup>2</sup>
	Orientation	S <sub>1</sub>	S <sub>2</sub>	
Borehole 1:				
3 . . . . .	4	17	16	Poor.
4 . . . . .	3	14	14	Acceptable.
5 . . . . .	4	20	19	Poor.
6 . . . . .	1	1	1	Excellent.
21 . . . . .	25	39	30	Bad.
22 . . . . .	5	18	17	Poor.
23 . . . . .	3	6	6	Good
Borehole 2:				
24 . . . . .	3	9	10	Good.
25 . . . . .	1	3	3	Excellent.
26 . . . . .	2	7	7	Good.
27 . . . . .	1	1	1	Excellent.
28 . . . . .	1	1	1	Excellent.
Borehole 3:				
7 . . . . .	4	12	12	Acceptable.
8 . . . . .	2	4	4	Good.
9 . . . . .	7	20	19	Bad.
10 . . . . .	14	17	20	Bad.
11 . . . . .	6	26	25	Bad.
Borehole 4:				
12 . . . . .	3	12	13	Acceptable.
13 . . . . .	16	35	35	Bad.

<sup>1</sup>See text footnote 3 for explanation of S<sub>1</sub> and S<sub>2</sub>.

<sup>2</sup>See table 4.

Table 6.—Measurement quality as classified by strain screen

Doorstopper cell	Strain test				Quality
	Summation, $\mu\epsilon$		Difference		
	$\pm 45^\circ$	Horizontal + vertical	$\mu\epsilon$	pct	
Borehole 1:					
3 . . . . .	1,347	1,652	<b>305</b>	15	( <i>h</i> )
4 . . . . .	2,017	2,316	299	13	( <i>h</i> )
5 . . . . .	1,536	1,922	<b>386</b>	20	( <i>h</i> )
6 . . . . .	1,021	1,030	9	1	( <i>h</i> )
21 . . . . .	1,050	1,415	<b>365</b>	<b>26</b>	( <i>h</i> )
22 . . . . .	3,678	4,326	<b>648</b>	15	( <i>h</i> )
23 . . . . .	1,155	1,099	56	5	( <i>h</i> )
Borehole 2:					
24 . . . . .	1,220	1,335	115	9	( <i>h</i> )
25 . . . . .	1,744	1,704	40	2	( <i>h</i> )
26 . . . . .	2,606	2,760	154	6	( <i>h</i> )
27 . . . . .	2,960	2,984	24	1	( <i>h</i> )
28 . . . . .	1,848	1,867	19	1	( <i>h</i> )
Borehole 3:					
7 . . . . .	1,638	1,869	231	12	( <i>h</i> )
8 . . . . .	5,087	4,936	151	3	( <i>h</i> )
9 . . . . .	2,216	1,849	<b>367</b>	17	( <i>h</i> )
10 . . . . .	1,772	2,034	262	13	( <i>h</i> )
11 . . . . .	711	937	226	<b>24</b>	( <i>h</i> )
Borehole 4:					
12 . . . . .	1,542	1,383	159	10	( <i>h</i> )
13 . . . . .	2,090	2,550	<b>460</b>	18	( <i>h</i> )

<sup>1</sup>Bad reading; test value was above limits.

<sup>2</sup>Good reading; both test values were below limits.

NOTE.—Numbers in bold indicate values outside test limits.

A widely used screen that is included in the STRESSs-OUT data-reduction program identifies outlying strains. These are strains that deviate substantially from the average and greatly increase the squared error of the least squares fit estimate of the stress field. The governing assumption in this approach is that outlier data points are attributable to error and are not real conditions. Outlier data can be examined by comparing the results of the screening procedure described earlier with the outlier elimination routine in STRESSsOUT. The strain screen was used to eliminate the same number of strain gauges as were eliminated in the strain-screening process, i.e., 7 doorstopper cells, or 28 gauges, about 37 pct of the total. The first 28 strain gauges selected by the STRESSs-OUT program as outliers are listed in bold italics in table 6 for comparison with range- and strain-screen-passed data sets. Only 12 strain gauges were eliminated by both outlier and strain screens. By comparison, if both of these screens were essentially random, the expected overlap in selections would be between 10 and 11 strain gauges. This independence suggests that the outlying strains were valid measurements.

Table 7.—Comparison of screen results

Doorstopper cell	Strain gauge orientation, $\mu\epsilon$				Quality	
	+45°	-45°	Vertical	Horizontal	Strain screen <sup>1</sup>	Range screen <sup>2</sup>
<b>Borehole 1:</b>						
3 .....	420	927	-369	2,021	Bad.	Poor.
4 .....	161	<b>1,856</b>	189	2,127	Good.	Acceptable.
5 .....	146	<b>1,390</b>	-155	2,077	Bad.	Poor.
6 .....	324	697	508	522	Good.	Excellent.
21 .....	495	555	503	912	Bad.	Bad.
22 .....	<b>2,720</b>	958	528	<b>3,798</b>	Bad.	Poor.
23 .....	666	489	214	885	Good.	Good.
<b>Borehole 2:</b>						
24 .....	85	1,135	748	587	Good.	Good.
25 .....	483	1,261	<b>1,473</b>	231	Good.	Excellent.
26 .....	592	<b>2,014</b>	<b>2,097</b>	663	Good.	Good.
27 .....	519	<b>2,441</b>	1,151	<b>1,833</b>	Good.	Excellent.
28 .....	465	1,383	775	1,092	Good.	Excellent.
<b>Borehole 3:</b>						
7 .....	-126	<b>1,764</b>	862	1,007	Good.	Acceptable.
8 .....	<b>1,216</b>	<b>3,871</b>	<b>2,597</b>	<b>2,339</b>	Good.	Good.
9 .....	288	<b>1,928</b>	713	1,136	Bad.	Poor.
10 .....	618	1,154	940	1,094	Good.	Bad. <sup>3</sup>
11 .....	563	<b>148</b>	928	<b>9</b>	Bad.	Bad.
<b>Borehole 4:</b>						
12 .....	346	<b>1,196</b>	227	<b>1,156</b>	Good.	Acceptable.
13 .....	459	<b>1,631</b>	841	<b>1,709</b>	Bad.	Bad.

<sup>1</sup>See table 6.<sup>2</sup>See table 5.<sup>3</sup>Only disagreement between strain and range screens.

NOTE.—Numbers in bold italics indicate a STRESSsOUT-screened strain reading.

## STRESS FIELD SOLUTION

Stress estimates were developed using stress concentration factors developed by Rahn (1984) and laboratory values of rock elastic properties [Young's modulus of 69 GPa (10 million psi) and Poisson's ratio of 0.1]. Stress field estimates for the full and variously screened data sets are presented in table 8 along with the best stress field estimate from the 4250-level measurement site. The

discrepancies between the 4250- and 5300-level measurements that prompted this study are preserved by solutions for data sets developed by all the screening methods. The best estimate probably arises from the most impartially screened data set. Thus, the authors have selected the strain-screened data set (estimate F in table 8) to represent the best solution. This solution is presented in map coordinates in table 9.

Table 8.—Stress field estimates

Stress component	Magnitude		Bearing	Plunge
	MPa	psi		
A. 4250-level best estimate:				
$\sigma_1$ .....	91	13,200	N 40° W	13°
$\sigma_2$ .....	55	7,900	S 41° W	33°
$\sigma_3$ .....	37	5,400	S 68° E	54°
$\sigma_v$ .....	45	6,600		
B. All data:				
$\sigma_1$ .....	126	18,300	S 65° W	23°
$\sigma_2$ .....	92	13,300	N 11° W	28°
$\sigma_3$ .....	68	9,800	S 58° E	52°
$\sigma_v$ .....	82	11,900		
C. Range-screen-passed data:				
$\sigma_1$ .....	143	20,800	S 83° W	36°
$\sigma_2$ .....	74	10,700	N 5° E	16°
$\sigma_3$ .....	67	9,700	S 65° E	49°
$\sigma_v$ .....	94	13,600		
D. Strain-screen-passed data (best estimate):				
$\sigma_1$ .....	135	19,600	S 80° W	34°
$\sigma_2$ .....	73	10,500	N 4° W	9°
$\sigma_3$ .....	69	10,000	S 81° E	54°
$\sigma_v$ .....	90	13,100		
E. STRESSsOUT-screen-passed data (outlying 28 gauges removed):				
$\sigma_1$ .....	93	13,600	S 84° W	27°
$\sigma_2$ .....	56	8,100	S 84° E	63°
$\sigma_3$ .....	55	8,000	S 3° E	5°
$\sigma_v$ .....	64	9,200		
F. Strain-screen-passed data with an additional eight outlying gauges removed:				
$\sigma_1$ .....	99	14,300	S 78° W	27°
$\sigma_2$ .....	62	9,000	S 24° E	23°
$\sigma_3$ .....	56	8,100	N 32° E	54°
$\sigma_v$ .....	65	9,500		

NOTE.—Empty cells in columns intentionally left blank.

Table 9.—Best estimate of stress field in map coordinate system

Stress component	Magnitude	
	MPa	psi
$\sigma_{ns}$ .....	74	10,700
$\sigma_{ew}$ .....	113	16,400
$\sigma_v$ .....	90	13,100
$\tau_{ns/ew}$ .....	7	1,100
$\tau_{ew/v}$ .....	-30	-4,400
$\tau_{ns/v}$ .....	-5	-700

## STRESS FIELD CHARACTERIZATION

The stress field at the measurement site is fully described by the in situ stress estimate in only the most ideal of cases. That is, the rock mass and stress field may be considerably more complex than the assumptions implicit in STRESSsOUT calculations at both doorstopper-cell and measurement-site scales. This section attempts to go beyond these assumptions to better characterize the stress field.

### DOORSTOPPER-SCALE ASSUMPTIONS

The rock immediately surrounding a doorstopper cell was assumed to be homogeneous, continuous, isotropic, and linearly elastic. A uniaxial compression test showed the rock to be linearly elastic, although some hysteresis at low loads was noted. The available information was not sufficient to determine whether there was any anisotropy of elastic properties, but rock samples inspected appeared to be isotropic and did not show any structure on the scale of a doorstopper cell. Homogeneity and continuity were fairly well ensured by carefully inspecting the borehole with a camera to detect and avoid fractures and bed interfaces. Thus, the doorstopper cells were probably mounted inside the thicker beds. However, there would be no way to tell if there were a fracture in the rock far enough from the doorstopper cell to elude detection but still close enough to affect the stress field around it.

### SITE-SCALE ASSUMPTIONS

Assumptions on the scale of the measurement site are particularly important when using two-dimensional cells, which are capable of measuring stress only on the face at the end of a borehole. This two-dimensional local stress field has three components, but it is determined by four components of the in situ stress field. Thus, the in situ components are underdetermined and additional information from boreholes in other directions are needed before in situ conditions can be estimated. Data from doorstopper cells in three nonparallel boreholes are necessary to estimate the three-dimensional stress state.

The least squares procedure followed in the previous section assumes that all doorstopper cells were installed in a homogeneous material experiencing uniform loading. Any deviations from the average of measured material properties or the stress field estimate are considered

random errors. The potential for real variability in stress field and/or rock mass properties throughout the measurement site raises two important issues: assessment of local stress field variability and the potential for sampling bias. Assessment of local stress variability is needed to determine if deviations from ideal conditions are significant to engineering design. That is, it must be determined whether the pattern and/or degree of stress variability is sufficient to create ground control problems, including rock bursting, if not dealt with explicitly. Furthermore, sampling procedures need to be evaluated in light of any stress field and/or rock property variations to ensure that a valid estimate of average stress conditions is attained.

### Local Stress Variability

The degree of local stress variability can be investigated by examining outlying measurements and the consistency of local stress measurements. Under ideal conditions, there should be little variability among doorstopper cells installed in a single borehole far from the influence of mine openings. Ideal conditions are rare. Thus, the evaluation process becomes an investigation of the validity, and reason for, outlying strain measurements.

Tests for outlying strains and measurement validity were developed earlier in the course of the average stress field estimation procedure. During this process, a discrepancy was noted between the strain and range screens that examined doorstopper cell self-consistency and the identification of outlying strain readings. This discrepancy is examined in greater detail in table 10. Of particular interest are the strain readings that are clearly self-consistent but also identified as outliers. These strains can be described as good outlying strains and appear to represent local conditions. Their existence suggests that real variations are present at this measurement site. The locations of good outlying strain measurements are indicated in table 10. Stress estimates for the set of good outlying strains (estimate B in table 11) and the remaining strains (estimate C in table 11) show considerable differences in magnitude but remarkably similar orientations. Both estimates show a strongly biaxial stress field, with the maximum principal stress ( $\sigma_1$ ) oriented roughly perpendicular to bedding. Since many doorstopper cells produced strains for both data sets, the spatial significance of this result is not clear.

Table 10.—Location and number of good outlying overcore strain measurements

Location <sup>1</sup>	Total number of gauges	Strain-screen-passed gauges	STRESSsOUT-screen-passed gauges	Gauges passing both screens	Good outlier gauges	Good outlier gauges, pct	Rock type
1a .....	16	8	7	5	2	29	Vitreous quartzite.
1b .....	12	8	2	2	0	0	Vitreous quartzite.
2 .....	20	0	6	0	6	100	Super-vitreous quartzite.
3 .....	20	8	9	3	6	67	Hard sericitic quartzite.
4 .....	8	4	4	2	2	50	Unknown.

<sup>1</sup>See figure 7.

Table 11.—Stress estimates exploring good outlying strain measurements

Stress component	Magnitude		Bearing	Plunge
	MPa	psi		
A. Strain-screen-passed data:				
$\sigma_1$ .....	135	19,600	S 80° W	34°
$\sigma_2$ .....	73	10,500	N 4° W	9°
$\sigma_3$ .....	69	10,000	S 81° E	54°
$\sigma_v$ .....	90	13,100		
B. Outlying strains only:				
$\sigma_1$ .....	188	27,300	S 73° W	34°
$\sigma_2$ .....	93	13,500	N 49° E	55°
$\sigma_3$ .....	76	11,100	S 22° E	7°
$\sigma_v$ .....	85	12,300		
C. Strain-screen-passed data with outlying strains removed:				
$\sigma_1$ .....	90	13,100	S 84° W	21°
$\sigma_2$ .....	55	7,900	S 34° E	51°
$\sigma_3$ .....	53	7,600	N 7° E	31°
$\sigma_v$ .....	59	8,500		

NOTE.—Empty cells in columns intentionally left blank

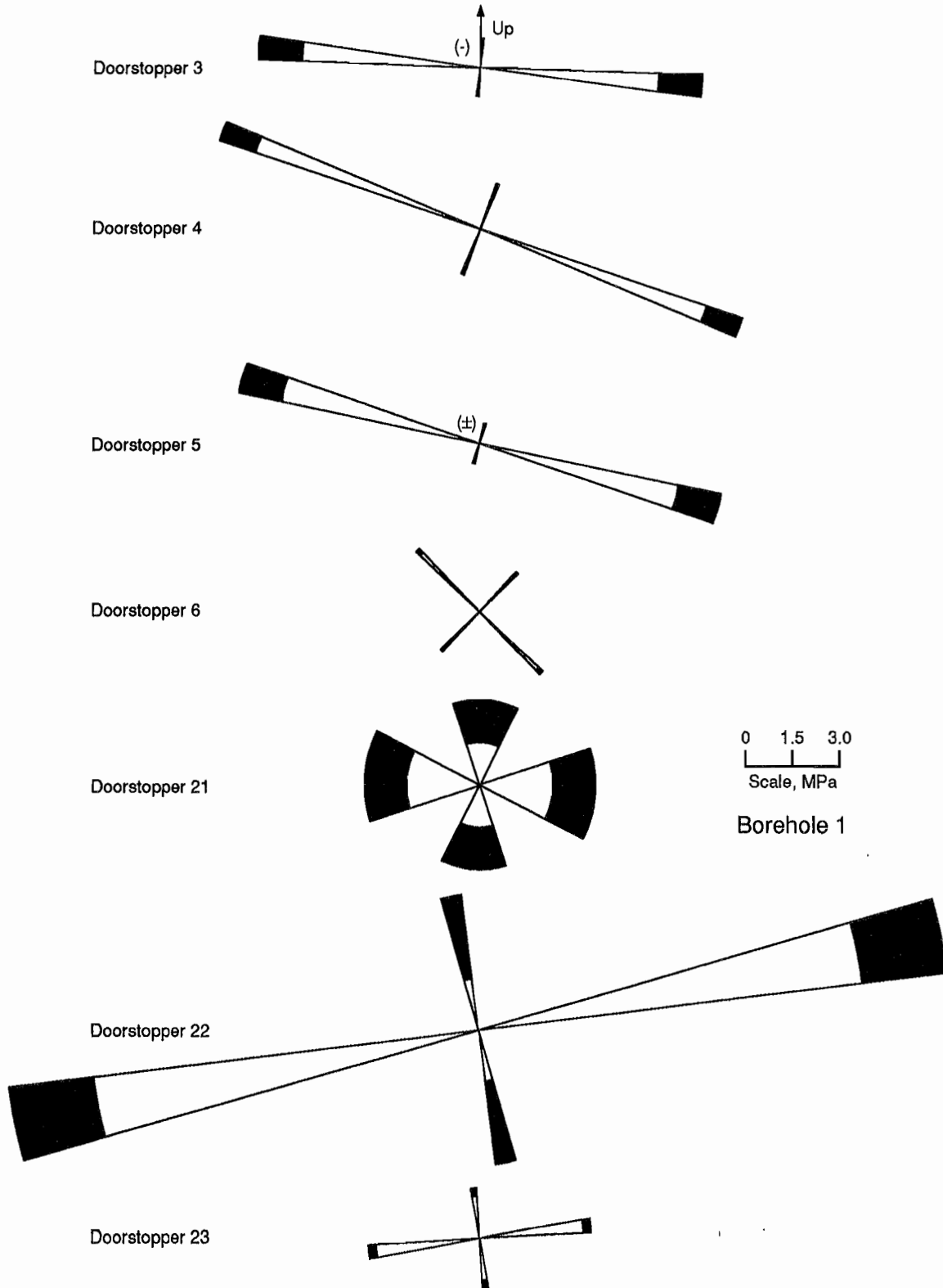
The spatial variation of stress can be examined more clearly by examining data from each borehole, and each doorstopper cell, as a unit. The influence of each borehole on the stress estimate can be evaluated by taking advantage of the extra borehole at the site to estimate stress using data from various combinations of three boreholes (table 12). The results show that removing data from boreholes 1, 2, and 4 (estimates B, C, D, and E, respectively; in table 12) nudges the estimates up, but removing borehole 3 data reduces the estimate. Significantly, though, the difference is primarily in the magnitude of stresses, not in rotation of the maximum principal stress direction.

The spatial variation of stress can also be examined within a borehole. The stress field on the end of the borehole at each doorstopper cell location ( $S_1$ ,  $S_2$ , and  $\theta$ ) can be estimated independently (appendix E). These solutions are plotted individually in figure 10 and summarized in figure 11. Large local variations in stress magnitude are evident in three of the four boreholes, although the high stress doorstopper cell in borehole 1 failed to make the

strain screen (in absolute, but not relative, terms). These variations may be showing changes in stress. Alternatively, they may be showing a homogeneous stress field with variations in elastic properties along the boreholes, or some combination of these alternatives. In any case, the assumption of a uniform rock mass under uniform loading is violated. The variation in borehole 2 is especially significant because it is repeated by two successive doorstopper cells. Local variations in stress direction are also evident in boreholes 1 and 2, but these variations do not correspond to variations in stress magnitude.

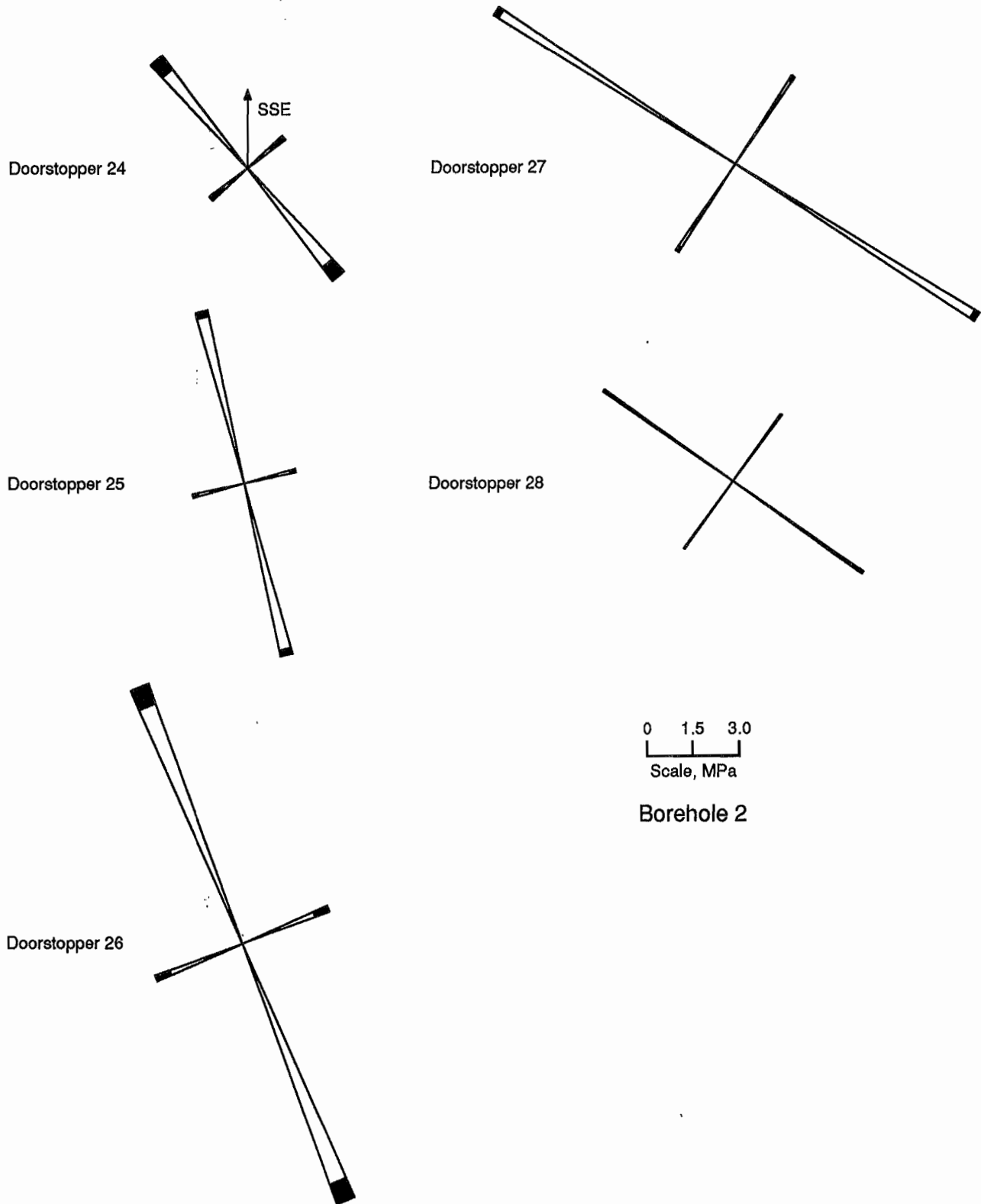
If all of the highly stressed doorstopper cells sample stress conditions caused by local but common mechanisms (hard inclusion effect in a stiff bed, etc.), a composite stress estimate can be developed. A similar approach might provide a view of the general background stress regime. For instance, doorstoppers 8, 22, 26, and 27 would be a solvable high stress data set while the remainder of cells could be assigned to an average or background set. Doorstopper 12 could be added to the high stress data set to include measurements from all four boreholes.

**Figure 10**



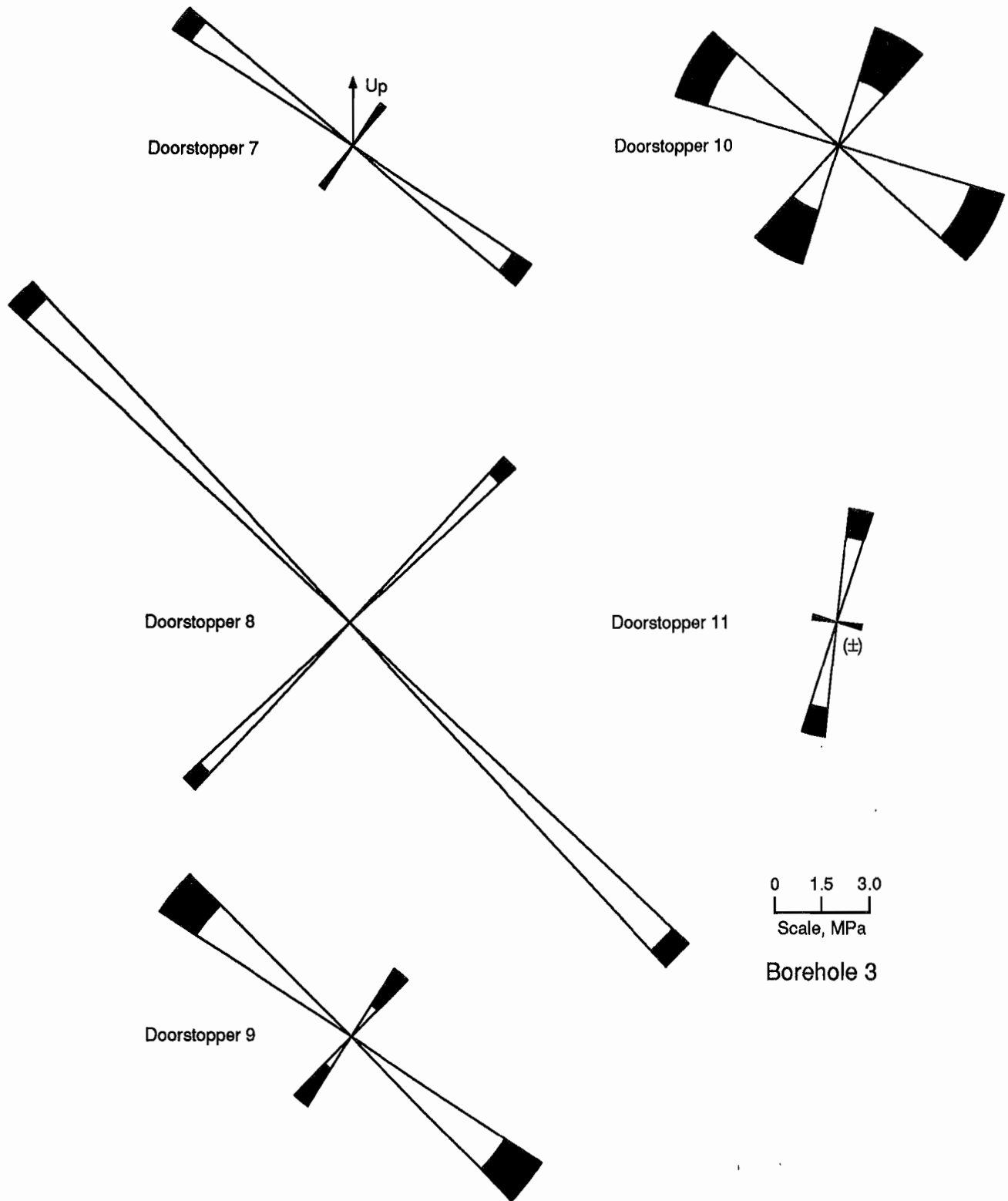
*Local stress field on end of borehole for each doorstopper cell. Plots show orientation of principal axes of stress ellipse. Boxes show ranges of magnitudes and orientations for each axis calculated from various combinations of three of four doorstopper strain gauges.*

Figure 10—Continued



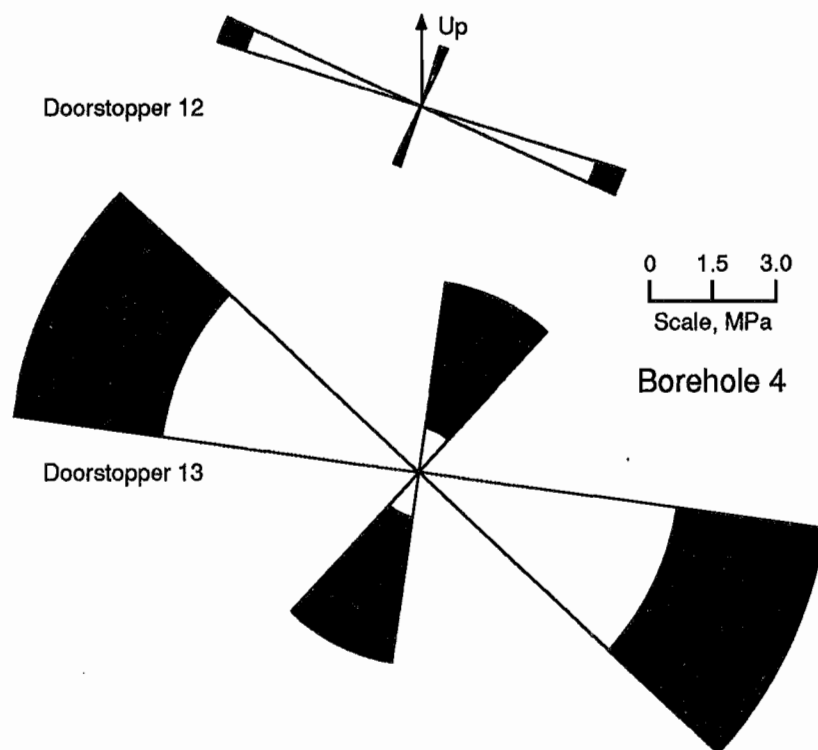
*Local stress field on end of borehole for each doorstopper cell. Plots show orientation of principal axes of stress ellipse. Boxes show ranges of magnitudes and orientations for each axis calculated from various combinations of three of four doorstopper strain gauges.*

Figure 10—Continued



*Local stress field on end of borehole for each doorstopper cell. Plots show orientation of principal axes of stress ellipse. Boxes show ranges of magnitudes and orientations for each axis calculated from various combinations of three of four doorstopper strain gauges.*

Figure 10—Continued



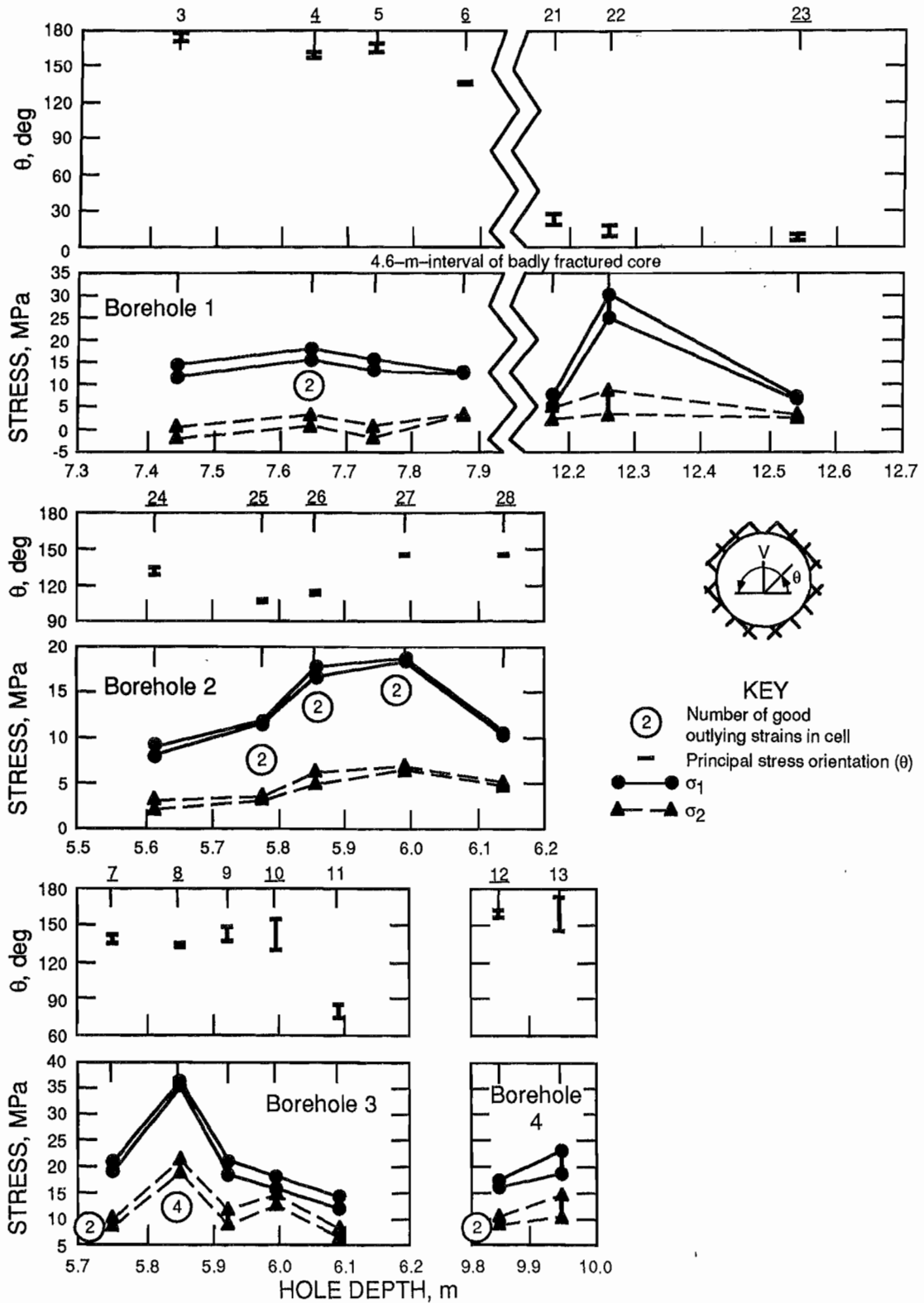
Local stress field on end of borehole for each doorstopper cell. Plots show orientation of principal axes of stress ellipse. Boxes show ranges of magnitudes and orientations for each axis calculated from various combinations of three of four doorstopper strain gauges.

Table 12.—Stress estimates developed from strain-screened data from various combinations of three of four boreholes

Stress component	Magnitude		Bearing	Plunge
	MPa	psi		
<b>A. Strain-screen-passed data:</b>				
$\sigma_1$ .....	135	19,600	S 80° W	34°
$\sigma_2$ .....	73	10,500	N 4° W	9°
$\sigma_3$ .....	69	10,000	S 81° E	54°
$\sigma_v$ .....	90	13,100		
<b>B. Strain-screen; borehole 1 data removed:</b>				
$\sigma_1$ .....	145	21,000	S 75° W	44°
$\sigma_2$ .....	81	11,800	S 50° E	31°
$\sigma_3$ .....	59	8,600	N 20° E	31°
$\sigma_v$ .....	106	15,400		
<b>C. Strain-screen; borehole 2 data removed:</b>				
$\sigma_1$ .....	161	23,400	N 84° W	28°
$\sigma_2$ .....	113	16,300	S 6° E	20°
$\sigma_3$ .....	81	11,800	N 53° E	54°
$\sigma_v$ .....	103	15,000		
<b>D. Strain-screen; borehole 3 data removed:</b>				
$\sigma_1$ .....	113	16,400	S 72° W	18°
$\sigma_2$ .....	68	9,900	S 32° E	14°
$\sigma_3$ .....	57	8,300	N 31° E	67°
$\sigma_v$ .....	63	9,100		
<b>E. Strain-screen; borehole 4 data removed:</b>				
$\sigma_1$ .....	140	20,300	S 85° W	36°
$\sigma_2$ .....	77	11,200	N 21° E	31°
$\sigma_3$ .....	61	8,900	S 41° E	39°
$\sigma_v$ .....	93	13,400		

NOTE.—Empty cells in columns intentionally left blank.

Figure 11



Local stress field on end of borehole summarized from results plotted in figure 10. Underlined numbers indicate stopper cells that passed strain screen. Circled numbers indicate number of good outlying strains for each doorstopper cell.

The resulting stress estimates (table 13) show a surprising decoupling of stress fields and the only marked change in stress direction noted in any of the alternative stress estimates. The high stress estimate, with and without doorstopper 12, has rotated  $\sigma_1$  to the northwest-southeast while dramatically increasing stress magnitudes.

The background or average stress estimate has rotated further to the southwest-northeast and is lower in magnitude. The lesser principal and vertical stress components are still significantly greater than the 4250-level estimate, but the greatest principal stress estimate at this level is not supportable by the background stress estimate. That is, the northwest component of the background stress estimate ( $\sigma_2$ ) is about 25 pct less than the northwest component of the 4250-level stress estimate ( $\sigma_1$ ). However, a weighted average of these two stress field estimates could easily carry the necessary stress.

It is clear that significant local variations in overcore strains were measured. Moreover, these strains had a significant impact on the stress field estimate. The next logical step in this analysis might be to develop a test site model as was attempted in part 1 of this series (Whyatt and Beus, 1995) for the 4250-level measurement site. However, there is not enough physical property information to differentiate between variations in overcore strain arising from changes in rock properties from those variations reflecting a true change in stress regime.

### Sampling

Estimation of a true average stress field for this site is seriously complicated by the presence of real variations in

stress and/or rock properties. The spatial distribution of measurements was not a great concern as long as each measurement could be considered an independent, randomly selected data point. But now that spatial dependence of stress and/or material properties has been established, increased attention must be paid to the actual position of measurements.

The measurable and unmeasurable sections in each borehole are shown in figure 5. Doorstopper core recovery requirements disqualified a large portion of each borehole. Whether fractures in the core were preexisting features or were caused by drilling is unclear. (Core discing was ruled out by the shape of core fragments.) In either case, the unmeasured sections probably represent zones of relatively weak, soft rock with relatively lower levels of stress.

Obviously, then, measurements at this site were concentrated in space. For example, seven measurements in borehole 1 were concentrated in two short sections comprising only 0.8 m (2.5 ft) of the available 10 m (30 ft). Furthermore, a plot of the competent borehole sections on a geologic map suggests that the five measured borehole segments actually measured conditions in only three stratigraphic intervals (figure 7). Thus, this measurement was clearly biased by concentrated sampling. This biased sampling could easily account for at least part of the unusually high stress levels, especially the unusually high magnitude of the vertical component.

Table 13.—Stress estimates from high stress and average stress data sets

Stress component	Magnitude		Bearing	Plunge
	MPa	psi		
A. Strain-screen-passed data:				
$\sigma_1$ .....	135	19,600	S 80° W	34°
$\sigma_2$ .....	73	10,500	N 4° W	9°
$\sigma_3$ .....	69	10,000	S 81° E	54°
$\sigma_v$ .....	90	13,100		
B. High stress data set only:				
$\sigma_1$ .....	299	43,300	N 22° W	48°
$\sigma_2$ .....	231	33,500	S 60° W	7°
$\sigma_3$ .....	70	10,100	S 35° E	41°
$\sigma_v$ .....	200	29,000		
C. High stress data set plus data from doorstopper 12:				
$\sigma_1$ .....	214	31,000	S 63° E	8°
$\sigma_2$ .....	167	24,300	N 12° W	63°
$\sigma_3$ .....	120	17,400	S 31° E	26°
$\sigma_v$ .....	159	23,100		
D. Average stress data set:				
$\sigma_1$ .....	100	14,500	S 48° W	25°
$\sigma_2$ .....	73	10,600	N 35° W	15°
$\sigma_3$ .....	55	8,000	N 84° E	60°
$\sigma_v$ .....	64	9,300		

NOTE.—Empty cells in columns intentionally left blank.

## DISCUSSION AND CONCLUSIONS

The stress estimate derived from the 5300-level overcore measurement site has been considered suspect, at first glance, by a number of researchers active in the Coeur d'Alene Mining District, including the authors, for three reasons. First, the large magnitude of  $\sigma_1$  does not fall in line with previous measurements in the district. Second, the rotation of  $\sigma_1$  from the generally accepted northwest quadrant to essentially east-west does not correlate with previous measurements in the district or the generally accepted view of recent right-lateral movement on the east-west trending Osburn Fault (Hobbs and others, 1965). Third, the estimate of vertical stress is greater than twice the overburden weight.

However, careful review and screening of the overcore strain data demonstrated that the measurements were valid and accurate. Furthermore, the unusual concentration of rock bursts suggested that the rock originally contained an unusually high density of elastically stored energy. This is possible considering the unusually strong, stiff rock at the site. At the same time, however, these stress levels do not appear to be representative of the overall stress condition at the mine.

The crux of the problem with this measurement, then, is proper interpretation of these good overcore strain measurements. Application of the conventional approach to analysis of these data encounters some serious problems. For instance, there is substantial evidence that the site was not homogeneous in either material properties or stress field. Furthermore, the apparent sampling bias toward strong, stiff rock probably increased stress estimate magnitudes. Integration of a more sophisticated rock property and in situ stress model into the analysis could account for these factors. Two such models were proposed and used to explore alternative stress estimates for the 4250-level measurement site in part 1 of this series (Whyatt and Beus, 1995). Unfortunately, expectations of a uniform site for this measurement led to insufficient attention to geologic information, and laboratory testing of rock samples was neglected. Thus, it is not practical to pursue alternative models for this site.

Based on the available information, the best estimate of stress conditions at the measurement site is given in table 14.

All indications are that these measured stresses did exist, at least locally, and were the driving force behind the unusually severe rock-burst activity. The contrasts in rock elastic properties and the proximity of the site to the axis of the Hook anticline and a fault provide more than

sufficient opportunity for the development of a complex natural stress field. Energy calculations show that the extent of local stress concentrations could be quite limited, on the order of only a hundred or so cubic meters, and still contain sufficient strain energy to power the three major rock bursts on January 10, 17, and 18, 1990. The stress field rotation was remarkably stable throughout the screening and sorting processes, and may well exist throughout the site. However, decomposition of the strain data into high stress and average stress data sets, and apparent rotation of stress orientations in two of the boreholes suggest that stress orientation is locally variable, at least to a small degree. This apparent rotation of the overall stress field should be apparent in the geomechanical behavior of surrounding mine openings. Some indications of a stress field rotation have been noted in bored raises near the axial plane of the Hook anticline. These indications and the relationship of this stress measurement to mine-wide stress conditions are explored in part 4 (Whyatt and others, 1995) of this series of reports.

Table 14.—Best estimate of average stress conditions at measurement site

Stress component	Magnitude		Bearing	Plunge
	MPa	psi		
$\sigma_1$ .....	135	19,600	S 80° W	34°
$\sigma_2$ .....	73	10,500	N 4° W	9°
$\sigma_3$ .....	69	10,000	S 81° E	54°
$\sigma_v$ .....	90	13,100		

NOTE.—Empty cells in columns intentionally left blank.

This overcore stress measurement suggests that localized stress concentrations in a natural stress field were associated with a concentration of rock-burst activity that interfered with excavation of development openings. Similar observations between natural and excavation-induced stress concentrations and rock bursts have been reported throughout the world. Further work needs to be done to identify which geologic structures and strata are prone to naturally concentrating stress to a degree sufficient to cause rock bursts at the Lucky Friday Mine. This information could then be used to place development openings in relatively rock-burst-safe portions of the rock mass. Finally, it is clear that overcore stress measurements in the Lucky Friday Mine should not be considered to be routine tests. Rather, each measurement should be approached as a geomechanical experiment in a complex rock mass.

Interpretation of in situ stress at the site was hampered by the limited information collected on rock properties as part of the measurement effort. But the information indicates that some assumptions implicit in the stress estimation procedure were violated. In the future, widespread and thorough testing of rock properties and mapping of geologic structure should be carried out, especially if a heterogeneous site is suspected. Analysis of available information showed that while violations of underlying assumptions were sufficient to erode confidence in the stress measurement, they were not sufficient to explain the

tremendous difference between measured and expected values. Furthermore, stress estimation techniques for doorstopper cells and other two-dimensional cells need to be developed in which more sophisticated site models are incorporated to allow for variations in physical properties and stress. Additional research on the type and degree of natural stress variations that can be expected in typical geologic settings would also be useful for developing site models and evaluating the difficulty of estimating stress at potential overcore sites.

## ACKNOWLEDGMENTS

The authors wish to express their appreciation to the staff of Hecla Mining Co., Lucky Friday Unit, Mullan, ID, and especially to George Johnson, mine manager; Steve Lautenschlager, mine superintendent; Rich Appling, mining engineer; and Ed Wilson, head of the safety department, for providing a location for the field work, logistics support, and a safe working environment.

The authors also wish to thank those at the Spokane Research Center (SRC) who assisted in the drilling and measurement work at the Lucky Friday Mine: Mike Jones, Gene Stone, and Mike King, electrical engineers; Bob McKibbin, general engineer; and Ted Williams and Jeff Johnson, mining engineers. Jeff Johnson's detailed field notes and laboratory tests were particularly useful.

We also acknowledge the invaluable contributions of our USBM colleagues Brad Seymour, mining engineer, and Priscilla Wopat, technical publications editor, in reviewing and improving this manuscript. The assistance of Mark Larson, mining engineer, and Kylan Kracher, engineering technician, both of SRC, were a great help in conducting computer analyses of overcore strains and mining-induced stress. The guidance and support of Charles Fairhurst, professor of civil engineering, University of Minnesota, Minneapolis, MN, and Mel Poad, group supervisor, SRC, are also gratefully acknowledged.

## REFERENCES

- Allen, M. Determining the In-Situ Stress Field on the 4250 Level in the Lucky Friday Mine: Using the CSIR Biaxial Strain Gage and Structural Geologic Mapping. M.S. Thesis, Univ. ID, Moscow, ID, 1979, 73 pp.
- Beus, M. J., and S. S. M. Chan. Shaft Design in the Coeur d'Alene Mining District, Idaho—Results of In Situ Stress and Physical Property Measurements. USBM RI-8435, 1980, 39 pp.
- Chan, S. S. M. A Case Study of In-Situ Rock Deformation Behavior for the Design of Ground Support System. USBM OFR 44-73, 1972, 130 pp.; NIIS PB 221 880/AS.
- Goodman, R. E. Introduction to Rock Mechanics. John Wiley, 1980, pp. 121-123.
- Gutenberg, B., and C. F. Richter. Magnitude and Energy of Earthquakes. *Ann. Geofis. (Rome)*, v. 9, 1956, pp. 1-15.
- Hedley, D. G. F. Rockburst Handbook for Ontario Hardrock Mines. CANMET Spec. Rep. SP92-1E, 1992, 305 pp.
- Hobbs, S. W., A. B. Griggs, R. E. Wallace, and A. B. Campbell. Geology of the Coeur d'Alene District, Shoshone County, Idaho. U.S. Geol. Surv. Prof. Pap. 478, 1965, 139 pp.
- International Society for Rock Mechanics. Suggested Methods for Rock Stress Determination. *Int. J. Rock Mech. Min. Sci. Geomech. Abstr.*, v. 24, No. 1, 1987, pp. 53-74.
- Jenkins, M., and R. McKibbin. Practical Considerations of In Situ Stress Determination. Paper in Proceedings, International Symposium on Application of Rock Characterization Techniques in Mine Design, ed. by M. Karmis. *Soc. Min. Eng.*, 1986, pp. 33-39.
- Larson, M. K. STRESsOUT—A Data Reduction Program for Inferring Stress State of Rock Having Isotropic Material Properties: A User's Manual. USBM IC 9302, 1992, 163 pp.
- Leighton, F. A Case Study of a Major Rock Burst. USBM RI 8701, 1982, 14 pp.
- McMahon, T. Rock Burst Research and the Coeur d'Alene District. USBM IC 9186, 1988, 45 pp.
- Pariseau, W. G., J. K. Whyatt, and T. J. McMahon. Rock Mechanics Investigations at the Lucky Friday Mine (In Three Parts): 3. Calibration and Validation of a Slope-Scale, Finite-Element Model. USBM RI 9434, 1992, 16 pp.
- Rahn, W. Stress Concentration Factor for the Interpolation of "Doorstopper" Stress Measurements in Anisotropic Rocks. *Int. J. Rock Mech. Min. Sci. Geomech. Abstr.*, v. 21, No. 6, 1984, pp. 313-326.
- Scott, D. F. Geologic Investigations Near an Underhand Cut-and-Fill Stope, Lucky Friday Mine, Mullan, ID. USBM RI 9470, 1993, 21 pp.
- Skinner, E. H., G. G. Waddell, and J. P. Conway. In Situ Determination of Rock Behavior by Overcore Stress Relief Method, Physical

Property Measurements, and Initial Deformation Method. USBM RI 7962, 1974, 87 pp.

Spottiswoode, S. M., and A. McGarr. Source Parameters of Tremors in Deep-Level Gold Mine. Bull. Seismol. Soc. Am., v. 65, No. 1, 1975, pp. 93-112.

Whyatt, J. K. Geomechanics of the Caladay Shaft. M.S. Thesis, Univ. ID, Moscow, ID, 1986, 195 pp.

Whyatt, J. K., and M. J. Beus. In Situ Stress at the Lucky Friday Mine (In Four Parts): 1. Reanalysis of Overcore Measurements From 4250 Level. USBM RI 9532, 1995, 26 pp.

Whyatt, J. K., M. J. Beus, and M. K. Larson. In Situ Stress at the Lucky Friday Mine (In Four Parts): 3. Reanalysis of Overcore Measurements From the Star Mine. USBM RI, 1995a, in press.

Whyatt, J. K., T. J. Williams, and W. Blake. In Situ Stress at the Lucky Friday Mine (In Four Parts): 4. Mine In Situ Field. USBM RI, 1995b, in press.

Whyatt, J. K., T. J. Williams, and M. P. Board. Rock Mechanics Investigations at the Lucky Friday Mine (In Three Parts): 2. Evaluation of Underhand Backfill Practice for Rock Burst Control. USBM RI 9433, 1992a, 10 pp.

Whyatt, J. K., T. J. Williams, and W. G. Pariseau. Trial Underhand Longwall Stope Instrumentation and Model Calibration at the Lucky Friday Mine, Mullan, ID. Paper in Rock Mechanics Proceedings of the 33rd Symposium, ed. by J. R. Tillerson and W. R. Wawersik (June 3-5, 1992, Santa Fe, NM). Balkema, 1992b, pp. 511-519.

Williams, T. J., J. K. Whyatt, and M. E. Poad. Rock Mechanics Investigations at the Lucky Friday Mine (In Three Parts): 1. Instrumentation of an Experimental Underhand Longwall Stope. USBM RI 9432, 1992, 26 pp.

## APPENDIX A.—MINING-INDUCED STRESS AT OVERCORE SITE

The level of mining-induced stress at the measurement site was estimated with a MINSIM-D boundary-element model of the Lucky Friday Mine. Model runs conducted with an arbitrary in situ stress field and without backfill were used to generate the estimates of stress presented in table A-1. The magnitudes of stress components are less than 5 pct of horizontal in situ stress. Thus, mining-induced stress should not have a major influence on the measured in situ stress. Backfill, if included in the model, would reduce the estimate of mining-induced stress further.

Table A-1.—Mining-induced stress at measurement site

Stress component	In situ stress		Mining-induced stress without backfill	
	MPa	psi	MPa	psi
$\sigma_{xx}$ . . . . .	84.24	12,200	2.02	290
$\sigma_{yy}$ . . . . .	84.24	12,200	-0.20	-30
$\sigma_{xy}$ . . . . .	42.12	6,100	1.02	150
$\tau_{xy}$ . . . . .	0	0	-1.36	-200
$\tau_{yz}$ . . . . .	0	0	-1.52	-220
$\tau_{zx}$ . . . . .	0	0	-0.78	-110

NOTE.—Compressive strength is positive.

## APPENDIX B.—DRILLING NOTES ON GEOLOGY<sup>1</sup>

The following information was collected during borehole drilling and doorstopper cell installation at the Lucky Friday Mine. Measurements are provided in U.S. customary units because the original measurements were in inches and feet.

### Borehole 2 (up):

Argillite interbed just beyond doorstopper 24 striking about 30° to the borehole.

### Borehole 3 (right):

Doorstopper 9 was recovered with only a 1/4-in stub and had cubic pyrite crystals in the face of the stub. The next 6 in (21 ft, 4 in to 21 ft, 10 in) were "very fractured with closely-spaced micro joints. The rock is quartzite and looks solid."

### Borehole 4 (left):

Audible popping of rock along the borehole was noticed during pauses during drilling the initial section of the

borehole (0 to 30 ft). A fault zone was encountered at about 28 ft (25 to 30 ft). The borehole had to be cleaned of rock chips before installing the first doorstopper gauge. The borehole had been cleaned at the end of the previous week when the initial 30 ft of borehole had been completed.

The rock at doorstopper 12 (first in this borehole at 32 ft, 2-3/4 in) was described as "good rock" with 1/2- to 1-in pieces of core recovered.

A soft "talcy" fault paralleling the borehole was encountered with doorstopper 20 (36 ft).

Ambient borehole temperatures for overcoring the various boreholes were—

Borehole 4 (left), 100 °F.

Borehole 1 (center), 110 °F.

Borehole 3 (right), 110 °F.

Borehole 2 (up), 106 to 107 °F.

---

<sup>1</sup>Jeff Johnson, mining engineer at the USBM's Spokane Research Center, collected the information in this section.

## APPENDIX C.—ROCK PROPERTIES

Rock properties for the measurement site were estimated from geologic observations, laboratory tests on suitable surviving samples, and reports of laboratory testing of similar Revett Quartzite samples. Five samples saved from the field measurement program form the foundation for these estimates, all of which were glued to doorstopper cells. Two of these samples were large enough to provide test specimens for uniaxial compression testing. Information gleaned from these samples is summarized in table C-1. Observations of rock types are plotted by location in figures 5 and 7.

These properties are similar to those reported by Allen (1979) for sulfide-altered quartzite at the 4250 level. His results for three samples are given in table C-2.

Sericitic quartzite samples taken from the Revett Formation in the Crescent and Lucky Friday Mines were somewhat softer (table C-3). On the basis of these results, the hard sericitic quartzite was estimated to have a Young's modulus of 48 GPa (7 million psi) and a Poisson's ratio of 0.2. Elastic properties for each rock type and the site as a whole are estimated in table 2. A review of Coeur d'Alene rock properties, including all of these results, has been compiled by Whyatt (1986).

Table C-1.—Rock type and results of uniaxial compression tests

Doorstopper cell <sup>1</sup>	Young's modulus		Poisson's ratio	Strength		Density, g/cm <sup>3</sup>	Rock type
	GPa	10 <sup>6</sup> psi		MPa	psi		
3 .....	69	10	0.10	324	47,000	2.7	Vitreous quartzite.
7 .....	ND	ND	ND	ND	ND	ND	Hard sericitic quartzite.
10 .....	ND	ND	ND	ND	ND	ND	Hard sericitic quartzite.
23 .....	ND	ND	ND	ND	ND	ND	Vitreous quartzite.
28 .....	90	13	0.10	310	45,000	2.7	Super-vitreous quartzite.
Average .....	79	11.5	0.10	317	46,000	2.7	

ND No data.

<sup>1</sup>Sample recovered from numbered doorstopper cell.

Table C-2.—Measured rock properties of sulfide-altered quartzite, 4250 level, Lucky Friday Mine (after Allen, 1979)

Sample	Young's modulus		Poisson's ratio	Strength	
	GPa	10 <sup>6</sup> psi		MPa	psi
1 .....	65.5	9.5	0.14	470	68,300
2 .....	60.7	8.8	NR	415	60,200
3 .....	68.9	10	NR	460	66,700

NR Not reported.

Table C-3.—Properties of Revett Formation rocks from various locations in Coeur d'Alene Mining District

Site	Young's modulus		Poisson's ratio	Strength		Rock type	Reference
	GPa	10 <sup>6</sup> psi		MPa	psi		
Lucky Friday 4240 level	54.8	7.95	0.22	310	45,000	Sericitic quartzite.	Allen (1979).
Crescent 3300 level . . .	50.0	7.1	NR	185	26,900	Sericitic quartzite.	Skinner and others (1974).
Galena .....	50.3	7.3	0.27	224	32,500	Sericitic quartzite.	Chan (1972).
Galena .....	44.1	6.4	NR	116	16,800	Revett Quartzite.	Ageton (in Beus and Chan, 1980).
Galena .....	60.7	8.8	NR	290	42,000	Competent quartzite.	Royea (in Beus and Chan, 1980).
Galena .....	NR	NR	NR	199	28,800	Incompetent quartzite.	Royea (in Beus and Chan, 1980).

NR Not reported.

NOTE.—Poisson's ratio not measured in some test programs.

## APPENDIX D.—ROCK-BURST ELASTIC ENERGY RELEASE

The energy released by three rock bursts on January 10, 17, and 18, 1990, was not measured directly but can be estimated from a relationship between local magnitude ( $M_l$ ) and energy ( $W_k$ ) (equation D-1) below:

$$\log W_k = 1.5 M_l - 1.2. \quad (D-1)$$

This relationship was developed for California earthquakes (Gutenberg and Richter, 1956) and has been confirmed for mine tremors in the Republic of South Africa by Spottiswoode and McGarr (1975). Application of this relationship to the three large bursts at the measurement

site, assuming a local magnitude of 0.5 for the second burst, gives a total seismic energy release of approximately 12.3 MJ. A source energy of 19 to 37 MJ can be estimated using a seismic efficiency for strain bursts of 30 to 60 pct (Hedley, 1992).

The volume of rock destressed by these events can be estimated from equation D-2 (see below) if the source of energy is assumed to be primarily stored strain energy (Hedley, 1992). A strain energy density ( $\mu_M$ ) of approximately 0.17 MJ/m<sup>3</sup> is based on overcore and laboratory measurements of elastic rock properties. Depending on the seismic efficiency, these events destressed an estimated 100 to 200 m<sup>3</sup> (3,500 to 7,000 ft<sup>3</sup>) of rock.

$$U_M = \frac{1}{2E} \left[ \sigma_1^2 + \sigma_2^2 + \sigma_3^2 - 2\nu (\sigma_1\sigma_2 + \sigma_2\sigma_3 + \sigma_3\sigma_1) \right]. \quad (D-2)$$

## APPENDIX E.—DOORSTOPPER CELL LOCAL SOLUTIONS

Local deviation in stress field can be examined by developing independent stress estimates for each instrument location. The strain field measured at the *end* of a borehole by any combination of three of the four strain gauges can be converted to stress using Hooke's law

(for example, see Goodman, 1980). Local stress solutions are listed in table E-1 for various sets of three strain gauges for a Young's modulus of 6.9 GPa (1 million psi). The range of solutions is summarized in table E-2 and plotted in figures 10 and 11.

Table E-1.—Principal stress solutions for stress on end of borehole

Stress attributes <sup>1</sup>	Solution 1	Solution 2	Solution 3	Solution 4
<b>Doorstopper 3:</b>				
$\theta$ , deg . . . . .	171	173	178	175
$S_1$ , MPa . . . . .	14.37	11.97	14.01	13.68
$S_2$ , MPa . . . . .	-0.13	-0.36	-0.23	-2.07
<b>Doorstopper 4:</b>				
$\theta$ , deg . . . . .	157	157	162	161
$S_1$ , MPa . . . . .	17.97	15.47	16.84	16.76
$S_2$ , MPa . . . . .	1.99	1.92	3.12	0.63
<b>Doorstopper 5:</b>				
$\theta$ , deg . . . . .	162	163	169	167
$S_1$ , MPa . . . . .	16.23	13.02	15.16	14.95
$S_2$ , MPa . . . . .	0.34	0.22	1.41	-1.71
<b>Doorstopper 6:</b>				
$\theta$ , deg . . . . .	136	135	136	137
$S_1$ , MPa . . . . .	5.54	5.48	5.49	5.48
$S_2$ , MPa . . . . .	3.34	3.33	3.39	3.32
<b>Doorstopper 21:</b>				
$\theta$ , deg . . . . .	-23	-27	18	-2
$S_1$ , MPa . . . . .	7.79	4.74	7.57	6.76
$S_2$ , MPa . . . . .	4.41	4.31	4.63	2.30
<b>Doorstopper 22:</b>				
$\theta$ , deg . . . . .	9	17	18	12
$S_1$ , MPa . . . . .	28.57	24.93	30.32	28.20
$S_2$ , MPa . . . . .	8.72	6.77	6.97	3.51
<b>Doorstopper 23:</b>				
$\theta$ , deg . . . . .	10	7	5	8
$S_1$ , MPa . . . . .	6.78	7.13	6.70	6.82
$S_2$ , MPa . . . . .	2.70	2.83	2.78	3.14
<b>Doorstopper 24:</b>				
$\theta$ , deg . . . . .	131	128	130	134
$S_1$ , MPa . . . . .	9.13	8.37	8.48	8.28
$S_2$ , MPa . . . . .	2.37	2.14	3.03	2.24
<b>Doorstopper 25:</b>				
$\theta$ , deg . . . . .	105	106	107	106
$S_1$ , MPa . . . . .	11.50	11.63	11.62	11.83
$S_2$ , MPa . . . . .	3.19	3.40	3.07	3.21
<b>Doorstopper 26:</b>				
$\theta$ , deg . . . . .	114	111	111	114
$S_1$ , MPa . . . . .	18.02	17.36	17.40	16.73
$S_2$ , MPa . . . . .	5.77	5.11	6.39	5.74
<b>Doorstopper 27:</b>				
$\theta$ , deg . . . . .	145	144	145	145
$S_1$ , MPa . . . . .	18.79	18.59	18.66	18.64
$S_2$ , MPa . . . . .	6.94	6.92	7.07	6.88
<b>Doorstopper 28:</b>				
$\theta$ , deg . . . . .	144	144	145	145
$S_1$ , MPa . . . . .	10.89	10.74	10.79	10.77
$S_2$ , MPa . . . . .	5.21	5.19	5.31	5.16
<b>Doorstopper 7:</b>				
$\theta$ , deg . . . . .	137	134	138	141
$S_1$ , MPa . . . . .	14.17	12.50	12.84	12.59
$S_2$ , MPa . . . . .	1.92	1.62	3.27	1.52

See footnote at end of table.

Table E-1.—Principal stress solutions for stress on end of borehole—Continued

Stress attributes <sup>1</sup>	Solution 1	Solution 2	Solution 3	Solution 4
<b>Doorstopper 8:</b>				
$\theta$ , deg .....	132	134	132	131
$S_1$ , MPa .....	28.51	29.57	29.37	29.65
$S_2$ , MPa .....	14.04	14.29	13.18	14.21
<b>Doorstopper 9:</b>				
$\theta$ , deg .....	144	148	141	136
$S_1$ , MPa .....	11.83	14.78	13.86	14.27
$S_2$ , MPa .....	4.12	4.32	2.08	4.83
<b>Doorstopper 10:</b>				
$\theta$ , deg .....	140	129	150	154
$S_1$ , MPa .....	11.10	9.21	9.67	9.59
$S_2$ , MPa .....	6.43	6.07	7.86	5.69
<b>Doorstopper 11:</b>				
$\theta$ , deg .....	84	80	73	75
$S_1$ , MPa .....	6.74	6.57	7.26	5.39
$S_2$ , MPa .....	1.34	-0.43	0.82	0.74
<b>Doorstopper 12:</b>				
$\theta$ , deg .....	162	161	156	156
$S_1$ , MPa .....	9.29	10.61	9.90	9.94
$S_2$ , MPa .....	2.63	2.68	2.02	3.35
<b>Doorstopper 13:</b>				
$\theta$ , deg .....	151	145	173	165
$S_1$ , MPa .....	16.30	12.57	14.22	14.10
$S_2$ , MPa .....	5.68	5.44	7.77	3.92

<sup>1</sup>See text footnote 3.

Table E-2.—Range of individual doorstopper cell solutions for stress on end of borehole

Doorstopper cell	Orientation of $S_1$ , deg		$S_1$ , MPa		$S_2$ , MPa	
	Minimum	Maximum	Minimum	Maximum	Minimum	Maximum
<b>Borehole 1:</b>						
3 .....	171	178	11.97	14.37	-2.07	0.23
4 .....	157	162	15.47	17.97	0.63	3.12
5 .....	162	169	13.02	16.23	-1.71	1.41
6 .....	135	137	5.48	5.54	3.32	3.32
21 .....	-27	18	4.74	7.79	2.30	2.30
22 .....	9	18	24.93	30.32	3.51	8.72
23 .....	5	10	6.70	7.13	2.70	3.14
<b>Borehole 2:</b>						
24 .....	128	134	8.28	9.13	2.14	3.03
25 .....	105	107	11.50	11.83	3.07	3.40
26 .....	111	114	16.72	18.02	5.11	6.39
27 .....	144	145	18.59	18.79	6.88	7.07
28 .....	144	145	10.74	10.89	5.16	5.31
<b>Borehole 3:</b>						
7 .....	134	141	12.50	14.17	1.52	3.27
8 .....	131	134	28.51	29.65	13.18	14.29
9 .....	136	148	11.83	14.78	2.08	4.83
10 .....	129	154	9.21	11.10	5.69	7.86
11 .....	73	84	5.39	7.26	-0.43	1.34
<b>Borehole 4:</b>						
12 .....	156	162	9.29	10.61	2.02	3.35
13 .....	145	173	12.57	19.44	2.12	8.92